Anleitung zum Fortgeschrittenenpraktikum

Brownsche Molekularbewegung

Version vom 6. November 2018

UNIVERSITÄT
DES
SAARLANDES

Dr. Thomas John
Gebäude E2.6, Zimmer 3.23
☎ 0681 / 302 2944
✉ thomas.john@physik.uni-saarland.de

Inhaltsverzeichnis

1. Ziele des Praktikumsversuches 3

2. Ablauf, Vorarbeiten und vorbereitenden Fragen 3
   2.1. Ablauf des Praktikums 3
   2.2. Vorabreiten 4
   2.3. Vorbereitenden Fragen 4

3. Brownsche Molekularbewegung 5
   3.1. Freie Brownsche Molekularbewegung 5
   3.2. Molekularbewegung in einem optischen Potential 11
   3.3. Bewegung in einem aktiven Fluid 14

4. Experimenteller Aufbau 15
   4.1. Brown'sche Bewegung 15
   4.2. Optische Pinzette 15

5. Durchführung der Experimente 17
   5.1. Brown'sche Bewegung 17
   5.2. Optische Pinzette 18

6. Ausarbeitung und Auswertung 19

7. Literaturverzeichnis 20

Literatur 20

1. Ziele des Praktikumsversuches

Mit diesem Versuch soll Ihnen ein Einblick in die Brown'sche Molekularbewegung und den prinzipiellen Aufbau einer optischen Pinzette gegeben werden. Das Prinzip und die Umsetzbarkeit einer optischen Pinzette wurde 2018 mit dem Nobelpreis für Physik geehrt. Im letzten Teil des Versuches wird die stochastische Bewegung von Tracerpartikeln in einem aktiven Fluid untersucht. Diese setzt sich aus einem Brown'nschen und einen Anteil durch da aktive Fluid zusammen. Das aktive Fluid ist in unserem Fall eine Suspension von Mikroschwimmern. Die Mikroschwimmer werden die Algen *Chlamydomonas reinhardtii* sein, ein Standardschimmer für solche Untersuchungen. Solche Untersuchungen sind auch Gegenstand der aktuellen Forschung, siehe Anhänge, wobei noch nicht alle Fragestellungen zufriedenstellend verstanden sind.

Das detaillierte Verständnis der Brown'schen Molekularbewegung ist der Grundstein für die moderne Messmethode: Mikrorheologie. Mit dieser Methode können Materialparameter von komplexen Flüssigkeiten auf der Mikrometerskala erfasst werden. Dies ist insbesondere für heterogene Materialien von Interesse welche oft in biologischen Systemen vorliegen.

Die optische Pinzette ist eine Standardmethode zur kontaktfreien Manipulation kleiner Objekte geworden, z. B. für µm größer Kügelchen. Sie wird insbesondere bei biophysikalischen Experimenten häufig eingesetzt.

2. Ablauf, Vorarbeiten und vorbereitenden Fragen

2.1. Ablauf des Praktikums

Der Praktikumsversuch wird wie folgt ablaufen:

1. Als Vorbereitung auf den Versuch eignen Sie sich theoretisches Hintergrundwissen an. Die folgenden Vorarbeiten und das vorliegende Anleitungsmaterial werden Ihnen dabei behilflich sein.
2. Bereits vor Versuchsbeginn müssen Sie die Brown'sche Bewegung von 1 µm großen Kugeln in Wasser mit einem selbst erstellten Computerprogramm simulieren um eine Vorstellung über die zu erwartenden Größenordnungen zu erhalten.
3. In einem Vorgespräch unterhalten wir uns über die verwendeten Methoden, Auswertungen und beantworten ausstehende Fragen.

4. Im ersten experimentellen Teil werden Proben mit kleinen Kügelchen vorbereitet und die Brown'sche Bewegung ohne ein Potenzial im Mikroskop erfasst. Dabei werden wir wichtige Aspekte der Mikroskopie diskutieren. Aus den aufgezeichneten Folgen an Mikroskopbildern werden die Partikelpositionen als Funktion der Zeit ermittelt. Zur Auswertung der Daten werden statistische Kenngrößen aus diesen Zeitreihen extrahiert.

5. Im zweiten Teil lernen Sie die optische Pinzette und erfassen die Brown'sche Bewegung in einem Potential.

6. Im dritten, abschließenden Teil wird die die Brown'sche Bewegung in einer aktiven Flüssigkeit mit schwimmenden Algen erfasst.

2.2. Vorabreiten

Damit Sie die Experimente bereits während der Durchführung verstehen müssen Sie sich im Vorfeld ein Hintergrundwissen erarbeiten. In der Vorliegenden Anleitung finden Sie weitere Literaturquellen. Danach sollte es Ihnen leicht fallen, die vorbereitenden Fragen zu beantworten.

Des Weiteren sollen Sie als Vorarbeit mit einem selbst erstellten Computerprogramm die Brown'sche Bewegung eines 1 µm großen Partikels bei 20°C, mit der Dichte von Wasser in einer wässrigen Lösung simulieren und einige statistische Auswertungen an diesen Durchführen.

2.3. Vorbereitenden Fragen

1. Wer hat unabhängig von Einstein im Jahre 1906 eine Erklärung der Brown'schen Bewegung gegeben.

2. Wie lautet der letzte Satz in der Veröffentlichung von A. Einstein „Über die von der molekularkinetischen Theorie der Wärme geforderte Bewegung von in ruhenden Flüssigkeiten suspendierten Teilchen"

3. Wie lange dauert es, bei Vernachlässigung der Brown'schen Bewegung, bis Teilchen mit einem Durchmesser von 1 µm und einer Dichte von $1.05 \mathrm{g/cm^3}$ in einer Zelle mit der Höhe von 100 µm durch Sedimentieren auf den Boden abgesunken sind. Ist dieses Sedimentieren von solch kleinen Teilchen unter dem Einfluss der Brown'schen Bewegung weiterhin beobachtbar?

4. Was bedeutet der Begriff Ergodizität bei dynamischen Systemen?

5. Was sind Zeitmittel und Ensemble-Mittel bei der Berechnung der mittleren quadratischen Verschiebung aus den Partikel-Trajektorien? Können beide Mittlungen aus einem Satz an Trajektorien Verwendung finden? Wenn ja, wie wird dies numerisch durchgeführt?

6. Zur Bestimmung der Wahrscheinlichkeitsdichtefunktion aus den Verschiebungen den Partikelpositionen soll die Kerndichteschätzer-Methode verwendet werden. Was verbirgt sich hinter dieser Methode und welche Vorteile hat sie im Vergleich zur Erstellung von Histogrammen?

7. Nach welchem Prinzip funktioniert die Dunkelfeldmikroskopie im Vergleich zur Hellfeldmikroskopie?

8. Was ist die numerische Apertur eines Objektives und welchen Einfluss hat diese auf die Fallenstärke bei einer optischen Pinzette?

9. Welche Rolle spielt der Strahlungsdruck bei optischen Pinzetten?

10. Kann eine optische Pinzette auch mit vollständig transparenten Kügelchen betrieben werden?

11. Wer hat wann den Nobelpreis für Physik für die Umsetzung der optischen Pinzette erhalte?

12. Welchen Wert hat die Reynolds-Zahl für einen kugelförmigen Mikroschwimmer in Wasser, einen Durchmesser von 5 µm und eine Geschwindigkeit von 30 µm/s hat?

13. Bei einem plötzlichen Anhalten der Schwimmbewegung bewegt sich der Mikroschwimmer aufgrund seiner Trägheit und der Stokes'schen Reibung weiter. Erstellen Sie ein Diagramm wie die Abnahme der Geschwindigkeit über der Zeit dargestellt wird.

3. Brownsche Molekularbewegung

3.1. Freie Brownsche Molekularbewegung

Der Botaniker Robert Brown beobachtete im Jahre 1827 durch ein Mikroskop Pflanzenpollen in Wasser. Er erkannte, dass diese eine Zitterbewegung ausführen. Er vermutete, dass eine innewohnende Lebenskraft die Ursache war. Wie sich herausstellte, sind die Pollen jedoch nicht als lebende Objekte aktiv und an der Bewegung beteiligt, vielmehr werden sie von den umgebenden Wassermolekülen angestoßen. Nicht lebende Objekte führen diese Bewegung ebenfalls aus.

Eine detaillierte mathematische, physikalisch orientierte Beschreibung finden Sie z. B. in [1]. Das 2. Kapitel ist diesem Dokument anhängt.

Im Folgenden soll eine knappe Beschreibung der Brown'schen Bewegung gegeben werden. Die oben aufgeführten Pollenkörner können in erster Näherung als unelastische Kugeln angesehen werden. Die umgebenden Lösungsmittelmoleküle übertragen durch Stöße einen Impuls auf das Objekt, welcher auf der thermischer Energie der Moleküle beruht. Eine Änderung des Impulses der Lösungsmittelmoleküle und damit auch der kugelförmigen Objekte führt zu einer Kraft welche auf das Objekt wirkt. Da nun sehr viele Lösungsmittelmoleküle in einem kleinen Zeitintervall mit dem Objekt wechselwirken, bietet es sich an, im Experiment über zeitliche Mittelwerte zu sprechen. Da die Moleküle isotrop und unkorreliert mit dem Objekt wechselwirken, führt dieses eine zufällige Bewegung, einen sogenannten *random walk*, aus. Im zeitlichen Mittel über lange Zeiten, wirkt keine resultierende Kraft auf das Objekt, da die Kräfte in x-Richtung mit gleicher Wahrscheinlichkeit in $-x$-Richtung auftreten

$$\langle \vec{F}_{St}\,(t)\rangle = 0 \quad ; \quad \langle x\rangle = 0. \tag{1}$$

Außerdem kann für experimentell zugängliche Zeitskalen davon ausgegangen werden, dass die zeitliche Dauer der Wechselwirkung zwischen den Lösungsmittelmolekülen und dem Objekt unabhängig und δ-korreliert ist (siehe [1]):

$$\langle \vec{F}_i\,(t)\,\vec{F}_j\,(t')\rangle = \delta_{ij}\delta\,(t-t')\,. \tag{2}$$

Ohne Beschränkung der Allgemeinheit, wird im Weiteren nur eine Raumdimension betrachtet, da die Bewegungen der Objekte in den Raumrichtungen in unseren Betrachtungen vollständig voneinander entkoppelt sind. Die Darstellungen gelten für die verbleibenden Raumrichtungen ebenso. Die Bewegungsgleichung in einer Dimension für ein freies kugelförmiges Objekt in der Lösung, kann nun mit Hilfe der Stokes'schen Reibung und einer stochastischen Kraft wie folgt dargestellt werden:

$$F = m\ddot{x} = F_{St} - F_R = F_{St} - 6\pi\eta R\dot{x}. \tag{3}$$

Bei η handelt es sich um die dynamische Viskosität des Lösungsmittels, R ist der Radius des Objekts und $\dot{x}$ dessen stochastische Geschwindigkeit. Solche Differentialgleichungen für die Bewegung von Teilchen mit stochastischen Termen werden auch Langevin-Gleichungen genannt, nach Paul Langevin. Die Gleichung (3) kann umgeschrieben werden zu

$$mx\ddot{x} = m\left[\frac{d\,(x\dot{x})}{dt} - \dot{x}^2\right] = xF_{St} - 6\pi\eta Rx\dot{x}. \tag{4}$$

und somit

$$m\frac{d\,(x\dot{x})}{dt} = m\dot{x}^2 + xF_{St} - 6\pi\eta R_K x\dot{x}. \tag{5}$$

Die Mittelwertbildung ergibt

$$m\left\langle \frac{d\left(x\dot{x}\right)}{dt}\right\rangle = m\frac{d\langle x\dot{x}\rangle}{dt} = m\langle\dot{x}^2\rangle + \langle xF_{St}\rangle - 6\pi\eta R_K\langle x\dot{x}\rangle. \tag{6}$$

Nach Gleichung (3) verschwindet auch

$$\langle xF_{St}\rangle = \langle x\rangle\langle F_{St}\rangle = 0. \tag{7}$$

Außerdem gilt für die mittlere Energie des Teilchens das Äquipartitionstheorem (der Gleichverteilungssatz)

$$E_{kin} = \frac{1}{2}m\langle\dot{x}^2\rangle = \frac{1}{2}k_BT, \tag{8}$$

was mit Hilfe der Gleichungen (6) und (7) zu folgender Gleichung führt:

$$m\frac{d\langle x\dot{x}\rangle}{dt} = k_BT - 6\pi\eta R\langle x\dot{x}\rangle. \tag{9}$$

Es folgt daraus

$$\frac{1}{2}m\frac{d^2\langle x^2\rangle}{dt^2} + \frac{1}{2}6\pi\eta R\frac{d\langle x^2\rangle}{dt} = k_BT. \tag{10}$$

Diese Differentialgleichung beinhaltet keine stochastischen Größen mehr und Lösung für die variable Größe $\left\langle x^2\right\rangle(t)$ kann mit den Methoden der klassischen Analysis abgeleitet werden:

$$\left\langle x^2\right\rangle(t) = \frac{k_BT}{3\pi\eta R}t + C_1\frac{m}{6\pi\eta R}\mathrm{e}^{-\frac{6\pi\eta R}{m}t} + C_2. \tag{11}$$

Mit den Anfangsbedingungen $\left\langle x^2\right\rangle(0) = \left\langle\dot{x}^2\right\rangle(0) = 0$ ergeben sich die Integrationskonstanten $C_{1,2}$. Nur der lineare Term ist relevant für experimentell zugängliche Zeiten, siehe [1] Fig. 2.1 und es ergibt sich

$$\left\langle x^2\right\rangle(t) = 2Dt \quad \text{mit} \quad D = \frac{k_BT}{6\pi\eta R}. \tag{12}$$

Die Größe D wird als Diffusionskonstante bezeichnet, welche den direkten Zusammenhang mit der makroskopisch beobachtbaren Diffusion herstellt [2]. Die mittlere quadratische Verschiebung $\left\langle x^2\right\rangle$ mittelt sich im Gegensatz zu $\langle x(t)\rangle$ nicht aus und kann als typisches Merkmal der Brown'schen Bewegung angesehen werden[1]. Wenn auf das Kügelchen zusätzlich eine konstante Kraft angreift, so gibt es einen weiteren, deterministischen Term in der Bewegung, welcher aufgrund der Stokes'schen Reibung

[1] Im Falle der 3-dimensionalen Bewegung in einer isotropen Flüssigkeit ergibt sich: $\left\langle\vec{r}^2\right\rangle(t) = \left\langle x^2\right\rangle(t) + \left\langle y^2\right\rangle(t) + \left\langle z^2\right\rangle(t) = 2nDt \quad \text{mit} \quad n = 3.$

zu einer konstanten Geschwindigkeit führt, der Driftgeschwindigkeit $\vec{v}_{\text{Drift}}$. Da die anfängliche Beschleunigung des Kügelchens vernachlässigt werden kann spricht man von einer überdämpften Bewegung, siehe auch [3]. Die Vernachlässigung des Beschleunigungsterms wird auch aus der Lösung zu Problemstellung 3 im Kap. 2.3 deutlich. Es ergibt sich eine mittlere quadratische Verschiebung mit Drift für die x-Komponente:

$$\left\langle x^2 \right\rangle (t) = 2Dt + v_{\text{Drift},x}^2 t^2 \tag{13}$$

Vorbereitende Simulationen der Brownschen Bewegung 1:

Die numerische Simulation stochastischer Differentialgleichungen ist ein komplexes Feld in der Numerik. Im Falle der Brown'schen Bewegung im überdämften Regime vereinfacht sich diese auf die Summation von gaußverteilten Zufallszahlen. Zur Lösung der angegebenen Aufgaben empfehlen wir das Tutorial auf `http://experimentationlab.berkeley.edu/node/83` welches in MATLAB programmiert wurde. Eine kurze Einführung in Matlab finden Sie unter References auf dieser Webseite. Alternativ können Sie das frei verfügbare GNU Octave benutzen[2]

1. Simulieren Sie die eindimensionale Bewegung von Kügelchen mit einem Durchmesser von 1 µm in Wasser bei 20°C über einen Zeitram von 100 s mit einer Zeitauflösung von $\Delta t = 10\,\text{ms}$. Stellen Sie $x_n(t_i)$ und $x_n(t_i)^2$ für $n = 1 \ldots 5$ verschiedene Realisierungen des Rauschens in einer Abbildung dar.

2. Simulieren Sie selbige Kügelchen im zweidimensionalen Fall und stellen Sie die 5 Trajektorien als $y_n(x_n)$ dar. Diese Trajektorien stellen die Projektion einer dreidimensionalen Bewegung auf die $x-y$-Ebene dar, wie sie auch in den durchzuführenden Experimenten beobachtet werden.

3. Führen Sie beide Simulationen mit einer Driftgeschwindigkeit $\vec{v}_{\text{Drift}} = (0.1\,\mu\text{m/s}, 0)$ durch und stellen Sie diese dar.

Um im Experiment oder der numerischen Simulation die mittlere quadratische Verschiebung $\left\langle (x(t) - x(0))^2 \right\rangle$ der x-Komponente aus stochastischen Trajektorien zu ermitteln, muss über eine große Anzahl von Realisierungen gemittelt werden. Diese Mittlung wird Ensamble-Mittelung bezeichnet.

$$\text{Ensemble-Mittelung:} \quad \left\langle x^2 \right\rangle_{\text{E}} (t_i) = \frac{1}{n_{\max}} \sum_{n=1}^{n_{\max}} (x_n(t_i) - x_n(0))^2 \quad \text{mit} \quad x(0) = 0 \tag{14}$$

Vorbereitende Auswertung: Ensemble-Mittlung 2:

Simulieren Sie obige eindimensionale Bewegung für 100 Kügelchen und stellen Sie die berechnete mittlere quadratische Verschiebung, basierend auf einer Ensemble-Mittelung, dar, jeweils ohne Drift und mit Drift. Tragen Sie den erwarteten theoretischen Kurvenverlauf ebenfalls ein.

In realen Experimenten ist die Umsetzung vieler gleichartiger Realisierungen oft schwer umzusetzen. Daher wird oft die Ergodizität des Systems ausgenutzt. Wenn diese vorliegt, kann bereits aus einer einzelnen Trajektorie die mittlere quadratische Verschiebung berechnet werden. Diese Mittelung wird Zeit-Mittelung bezeichnet.

$$\text{Zeit-Mittelung:} \quad \left\langle x^2 \right\rangle_{\mathrm{t}} (\tau) = \frac{1}{i_{\max} - j} \sum_{i=1}^{i_{\max}-j} (x_{t_i+\tau} - x_{t_i})^2 \quad \text{mit} \quad \tau = t_j \tag{15}$$

Die Abb. 1 illustriert dieses Vorgehen. Dabei ist offensichtlich, dass diese Berechnung insbesondere für kleine Zeitintervalle einen genauen Mittelwert widerspiegelt, da bereits viele Terme in die Mittlung einfließen. Allerdings wird das berechnete $\left\langle x^2 \right\rangle_{\mathrm{t}}$ sehr ungenau für lange Zeitintervalle.

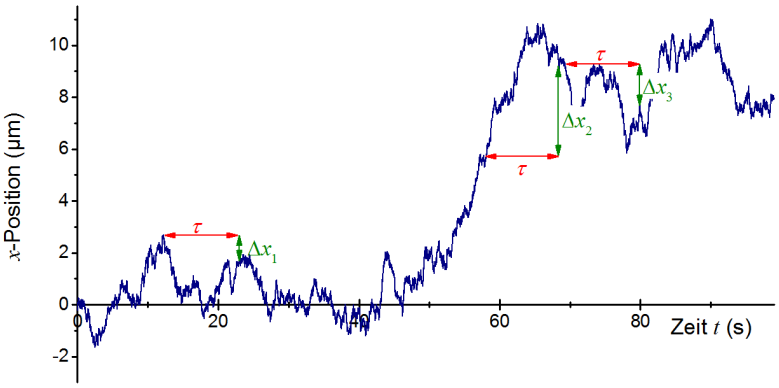

Abb. 1: Illustration der Berechung der mittleren quadratischen Verschiebung $\left\langle x^2 \right\rangle_{\mathrm{t}} (\tau)$ aus einer einzelnen Trajektorie mittels Zeitmittelung. Exemplarisch dargestellt für das feste Zeitintervall τ und drei verschienden Positionen innerhalb der Trajektorie. Die entgültige Mittelung erfolgt über alle möglichen Zeitintervalle innerhalb der Trajektorie.

Vorbereitende Auswertung: Zeit-Mittlung 3:

Simulieren Sie obige eindimensionale Bewegung für ein Kügelchen und stellen Sie die berechnete mittlere quadratische Verschiebung, basierend auf einer Zeit-Mittelung dar, jeweils ohne Drift und mit Drift. Eine doppeltlogarithmische Darstellung ist dabei sehr aussagekräftig. Tragen Sie den erwarteten theoretischen Kurvenverlauf ebenfalls ein.

Bei vielen Experimenten, wie auch unserem, liegt Ergodiziät vor. In solchen Fällen bietet es sich an, sowohl die Zeit- als auch die Ensamble-Mittelung durchzuführen.

Die mittlere quadratische Verschiebung wird auch mit MSD-*mean squared displacement* abgekürzt.

$$\mathrm{MSD}(\tau) = \left\langle \left\langle x^2 \right\rangle_{\mathrm{t}} \right\rangle_{\mathrm{E}}(\tau) = 2D\tau + v_{\mathrm{Drift},x}^2 \tau^2 \tag{16}$$

Neben dem MSD ist die Wahrscheinlichkeitsdichtefunktion der Kugelpositionen nach einem Zeitintervall τ ebenfalls ein wichtige Charakteristik der zufälligen Bewegung. Wenn die Partikel bei $t = 0$ an $x = 0$ starten, so ist diese *pdf-probability density function* für den eindimensionalen Fall gegeben durch, siehe auch [1] Gl. (2.39):

$$pdf(x, t|x = 0, t = 0) = \frac{1}{\sqrt{2\pi\sigma^2(t)}} \mathrm{e}^{-\frac{x^2}{2\sigma^2(t)}} \quad \text{mit} \quad \sigma^2(t) = 2Dt \tag{17}$$

Der senkrechte Strich in $pdf(x, t|x = 0, t = 0)$ trennt dabei die Variablen von ihren Anfangswerten. Dies stellt eine Gaussverteilung mit dem Schwerpunkt an $x = 0$ und der Standardabweichung $\sigma(t)$ beziehungsweise der Varianz $\sigma^2(t) = 2Dt$ dar. Beim Vorhandensein einer Driftgeschwindigkeit verschiebt sich die Gausverteilung mit $v_{\mathrm{Drift},x}t$. Das zweite Moment obiger Wahrscheinlichkeitverteilung ist zeitabhängig und identisch mit dem MSD(τ). Es beschreibt die die zeitliche Entwicklung der Breite dieser Verteilung:

$$\mathrm{MSD}(\tau) = \int_{-\infty}^{\infty} x^2 pdf(x, \tau) \mathrm{d}x \tag{18}$$

Für endliche Datensätze kann die zugrundeliegende Wahrscheinlichkeitsdichtefunktion, oft einfach Verteilung genannt, immer nur geschätzt werden. Eine weit verbreitete Methode um aus einem Datensatz die zugrundeliegende Wahrscheinlichkeitsdichtefunktion abzuschätzen ist die Erstellung eines Histogramms. Dieses sollte normiert sein, damit die Fläche unter dem Balkendiagramm 1 ergibt. Insbesondere bei kleinen Datensätzen sind Histogramme oftmals sehr verrauscht. Des Weiteren gibt es keine genaue Vorschrift, wie groß die Bin-Breite optimaler Weise zu wählen ist. In diesem Praktikumsversuch werden Sie eine weit aus elegantere Methode zur Bestimmung der pdf aus Datensätzen kennen lernen, die *Methode der Kerndichteschätzer*. Die Erläuterung der Methode finden Sie in der Wikipedia, insbesondere in der englischen Version, siehe `https://en.wikipedia.org/wiki/Kernel_density_estimation`. Wir beschränken uns auf Gaußkerne, was für stetige Verteilungen in den meisten Fällen eine gute Wahl ist. Die Breite h der Gaußkerne ist eine Entsprechung zur Bin-Breite bei Histogrammen. Im Gegensatz zu Histogrammerstellung existiert ein mathematischen Beweis, welcher eine optimale Kernbreite h vorgibt. Wenn ein Datensatz mit $x_i, i = 1 \ldots n$ Datenpunkten vorliegt und dieser Datensatz eine Standardabweichung $\hat{\sigma}$ hat, so ist die optimale

Schätzung der Gaußkernelbasierten pdf_K gegeben durch:

$$pdf_K(x) = \frac{1}{n}\sum_{i=1}^{n}\frac{1}{\sqrt{2\pi h^2}}\exp\left(-\frac{(x-x_i)^2}{2h^2}\right) \quad \text{mit} \tag{19}$$

$$h = \hat{\sigma}\sqrt[5]{\frac{4}{3n}} \quad \text{und} \quad \hat{\sigma} = \sqrt{\frac{1}{n}\sum_{i=1}^{n}(x_i-\bar{x})^2} \tag{20}$$

Aus der Definition ist bereits ersichtlich, dass diese Dichtefunktion auf 1 normiert ist, da die Fläche unter den einzelnen Gaußkern 1 ist. Des Weiteren ist diese Dichtefunktion glatt und somit differenzierbar. Dies spiegelt den physikalischen Ursprung dieser Dichtefunktion wider. Es ist wichtig zu verstehen, das die Wahl eines Gaußkerns nichts mit der zu erwartenden Gaußverteilung zu tun hat. Die Kerndichsteschätzermethode ist ein allgemeines numerisches Konzept für beliebige Verteilungen. Um dies zu veranschaulichen, führen Sie abschließend folgende freiwillige zusätzliche Auswertungen durch.

Auswertung: Schätzung der Wahrscheinlichkeitsdichtefunktion $pdf(x,t)$ 4:

freiwillige, vorbereitende Zusatzaufgabe

1. Erstellen Sie einen Datensatz aus 500 gleichverteilten Zufallszahlen im Intervall [0,1]. Berechnen Sie von diesem Sample ein normiertes Histogramm und vergleichen Sie dieses mit der berechneten Dichtefunktion nach der Methode der Kerndichteschätzer.

2. Simulieren Sie obige eindimensionale Bewegung für 500 Kügelchen bis $t = 1\,\mathrm{s}$. Erstellen Sie von den Endpositionen der Kügelchen wie obig ein normiertes Histogramm und eine $pdf(x, t = 1\,\mathrm{s})$ nach dem Kerndichteschätzer. Verwenden Sie eine logarithmische Skalierung der y-Achse. Tragen Sie die zu erwartende theoretische Verteilung in dieses Diagramm mit ein.

3.2. Molekularbewegung in einem optischen Potential

Funktionsweise einer optische Pinzette. Die optische Pinzette ist ein Werkzeug für einen schonenden, präzisen, nicht mechanischen Eingriff in ein System von kleinen, in Flüssigkeiten gelösten Objekten. Mit ihrer Hilfe können Kolloide an orten fixiert oder transportiert werden, sowie Kräfte im Piko-Newton-Bereich gemessen werden. Das Prinzip der Pinzette besteht in der Fokussierung einer intensiven elektromagnetischen Strahlung. Oft wird dabei infrarotes Licht verwendet, da Wasser für diese Wellenlängen fast keine Absorption aufweist. Intensiv bedeutet in diesem Falle, dass in der Praxis ein

LASER (Light Amplification by Stimulated Emission of Radiation) als Strahlungsquelle benutzt wird. Diese Strahlung wird durch eine Mikroskopobjektiv hoher numerischer Apertur auf einem Punkt in der Probe fokussiert. Dieser Punkt – der Fokuspunkt – stellt das Zentrum der optischen Falle dar. Hier entsteht ein dreidimensionales Potential, das in erster Näherung als harmonisch angesehen werden kann, da das Intensitätsprofil senkrecht zur Ausbreitungsrichtung der Strahlung (Grundmode TEM_{00}) gaußförmig und somit im Maximum annähernd harmonisch ist.

Die genauere theoretische Beschreibung zum besseren Verständnis der optischen Kräfte wird am Beispiel einer Kugel durchgeführt. Der Brechungsindex der zu fangenden Objekte muss größer als das n des umgebenden Mediums sein. Die Durchmesser $2R_k$ der Kugel im Vergleich zur verwendeten Laser-Wellenlänge λ ist entscheidend für die jeweiligen Vereinfachungen:

- Geometrische Optik ($2R_K \gg \lambda$):
  Exemplarisch kann die Strahlung auf das Objekt mit Hilfe von zwei einzelnen Teilstrahlen dargestellt werden. Wie in Abbildung 2 zu erkennen ist, werden die Strahlen A und B durch eine Linse in einem Punkt fokussiert. Treffen die Strahlen auf die Kugel, so wird dort das Licht gemäß dem Fresnel'schen Formeln sowohl beim Eintritt als auch beim Austritt gebrochen und ein Teil reflektiert. Bei kleinen Brechzahlunterschieden ist der reflektierte Anteil R relativ klein zum gebrochenen Anteil $T = 1 - R$. Nach dem Passieren der Kugel haben die Strahlen aufgrund der Brechung eine Netto-Richtungsänderung erfahren. Diese Richtungsänderung erfolgt bei beiden Strahlen In Richtung der Symmetrieachse des Systems. Mit dieser Richtungsänderung geht eine Impulsänderung der Photonen einher. Die kontinuierliche Impulsänderung führt zu einer Kraft F_A bzw. F_B auf das Kolloid. Die Superposition F_{AB} beschreibt die resultierende Kraft auf das Kolloid, welche immer zum Laserfokus gerichtet ist. Die Kraft pro Fläche, welche durch die Impulsänderung des reflektierten Lichtes R entsteht wird auch Strahlungsdruck oder Lichtdruck genannt. Er wirkt in Ausbreitungsrichtung des Lichtes und ist destabilisierend für die Falle. Demzufolge muss dieser Anteil klein für eine Stabile Falle.

- Mie-Regime ($2R_K \approx \lambda$):
  Der Bereich des Mie-Regimes stellt einen Übergangsbereich zwischen Rayleigh-Regime und geometrischer Optik dar. Dieser Bereich ist im Experiment am häufigsten anzutreffen. Der Wirkmechanismus ist analog obiger Stahlenoptik. Aufgrund der Welleneigenschaften des Lichtes treten Korrekturen in den jeweiligen Intensitäten auf. Die theoretische Berechnung der auftretenden Kräfte ist allerdings sehr komplex. Auf die genaue Ableitung wird hier verzichtet.

- Rayleigh-Regime ($2R_K \ll \lambda$):
  Die zu fangenden Objekte sind sehr viel kleiner als die Wellenlänge des benutzten

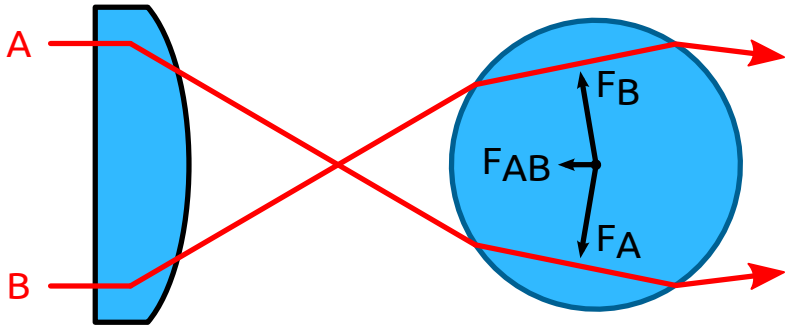

Abb. 2: Strahlengang durch die Objektivlinse des Mikroskops und einer transparenten Kugel, $n_{\text{Kugel}} > n_{\text{Medium}}$. Die resultierenden Kräfte aufgrund der gebrochenen Strahlen sind im Kugelzentrum angetragen. Die reflektierten Strahlen sind nicht eingezeichnet.

Lichtes. Die einfallende Strahlung kann vom Objekt reflektiert oder absorbiert werden, sodass die resultierende Kraft des Strahlungsdruckes auf dieses Objekt in Ausbreitungsrichtung der Strahlung gerichtet ist. Diese Kraft wird auch Streukraft genannt und destabilisiert die optische Pinzette. Wegen $2R_K \ll \lambda$ induziert das elektrische Feld des Laserlichtes einen elektrischen Dipol, welcher mit dem elektromagnetischen Feld des eingestrahlten Laserlicht wechselwirkt. Die so entstehende Kraft ist stets zum Ort größter Intensität gerichtet. Sie wird Gradientenkraft genannt und ist für die Fixierung des Objektes verantwortlich, sofern ihr Betrag die Stärke der Streukraft überkompensiert.

Molekularbewegung in einem optischen Potential. Das durch die optische Pinzette erzeugte, äußeres Potential kann in guter Näherung als harmonisch angesehen werden, wodurch sich die Bewegungsgleichung (3) für das Kolloid zu folgender Gleichung umschreiben lässt:

$$F = m\ddot{x} = F_{St} - F_R - F_P = F_{St} - 6\pi\eta R_K \dot{x} - kx. \tag{21}$$

Dabei beschreibt der Term kx eine Hooke'sche, linear rücktreibende Kraft der Pinzette, wobei der Faktor k ein Maß für die Fallenstärke darstellt. In der Praxis ist das betrachtete System durch das Lösungsmittel stark gedämpft, d.h. die Beschleunigungsterme sind gegenüber den Reibungstermen vernachlässigbar klein. Mit dieser Annahme ergibt sich die Langevin-Bewegungsgleichung der optischen Falle:

$$0 = F_{St} - 6\pi\eta R_K \dot{x} - kx. \tag{22}$$

Eine Vorhersage der Bewegung eines Brownschen Objektes in der optischen Pinzette ist auf Grund der stochastischen Kraft in der Bewegungsgleichung (22) nicht möglich. Eine Wahrscheinlichkeitsaussage auf Grund des thermischen Gleichgewichts kann aufgestellt

werden. In diesem stationären Gleichgewicht ist die Aufenthaltswahrscheinlichkeit des Kolloids Boltzmann-verteilt, das bedeutet:

$$pdf(x) \propto \exp\left(-\frac{U(x)}{k_B T}\right), \tag{23}$$

mit dem harmonischen Potential

$$U(x) = \frac{1}{2}k(x - x_0)^2 \tag{24}$$

Der funktionale Zusammenhang zwischen der Aufenthaltswahrscheinlichkeit und der Position in der optischen Falle kann mit einer Gaußschen Glockenkurve der Form

$$f(x) \propto \exp\left(-\frac{1}{2}\left(\frac{x - x_0}{\sigma}\right)^2\right), \tag{25}$$

angepasst werden, wobei σ die Standardabweichung ist. Vergleicht man die Koeffizienten aus Gleichung (23) und Gleichung (25), folgt:

$$k = \frac{k_B T}{\sigma^2}, \tag{26}$$

das heißt, durch Messung der Varianz σ^2 kann direkt die Fallenstärke k bestimmt werden.

3.3. Bewegung in einem aktiven Fluid

Als aktives Fluid wird eine Flüssigkeit außerhalb des thermischen Gleichgewichts bezeichnet, wobei aktive bewegende Partikel – natürlichen oder künstlichen Ursprungs – dem System kontinuierlich Energie zuführen. Es kommt zu einer Durchmischung der Flüssigkeit, zusätzlich zur Diffusion. Ein Beispiel für ein natürliches aktives Partikel stellt die Grünalge *Chlamydomonas reinhardtii* dar. Sie besteht aus einer einzelnen Zelle leicht oblater Form und ist zirka acht Mikrometer groß. Sie besitzt eine Augenfleck, um sich zur optimalen Photosynthese zu einer Lichtquelle zu positionieren. Dazu muss sich die Alge bewegen können. Dies erreicht sie durch zwei Flagellen, deren Schlagmuster den Armbewegungen eines Brustschwimmers gleicht. Da sie sich durch Schwimmen fortbewegt, wird sie auch als Mikroschwimmer bezeichnet. Das Schwimmen auf solch kleinen Längenskalen unterscheidet sich dramatisch von möglichen Schwimmbewegungen bei denen die Trägheit von Flüssigkeit und Schwimmer eine Rolle spielt, zum Beispiel bei uns Menschen. Die wichtige, dimensionslose Kennzahl -ohne physikalische Einheiten-, welche sich aus dem Verhältnis von Trägheitskräften zu dissipativen viskosen Kräften ergibt ist die Reynolds-Zahl. Eine sehr schöne Einführung in diese Thematik in dem Artikel [3] wiedergegeben. In diesem Praktikumsversuch werden Sie

eine Lösung obiger Grünalgen mit 1 µm kleinen Plastikkügelchen versetzen. Durch die zusätzliche Durchmischung wird sich die stochastische Bewegung der Kügelchen verändern. Diese Veränderung werden Sie mit den obig dargestellten Methoden zur Brown'schen Bewegung charakterisieren.

4. Experimenteller Aufbau

4.1. Brown'sche Bewegung

Die Untersuchungen zur reinen Brown'schen Bewegung und zur Bewegung in einer aktiven Flüssigkeit werden an einem selbstgebauten Mikroskop auf einem optischen Tisch durchgeführt. Dabei wird auch die Dunkelfeldmikroskopie angewendet welche auf der Streuung von Licht basiert. Diese Methode zeigt einen deutlich erhöhten Kontrast gegenüber der Hellfeldmikroskopie, welche auf Absorbtion basiert. Die Abb. 3 Abb. 4 verdeutlicht dieses. Der gesamte Versuchsaufbau ist sehr kompakt und leicht zugänglich gehalten. Dadurch ist es Ihnen möglich, im Bedarfsfall selbst die Justage der optischen Komponenten durchzuführen. Wie in Abbildung 3 zu erkennen ist, sind nur wenige Komponenten erforderlich: verschiedene Objektive für die unterschiedlichen Messungen, eine CCD-Kamera und eine Beleuchtungseinheit zur Visualisierung der Probe und zur Videoaufzeichnung, sowie ein motorisierter x-y-z-Tisch zur Fokussierung und Verschiebung der Probe.

4.2. Optische Pinzette

Für die optische Pinzette wird ein kommerzielles Mikroskop von Nikon verwendet in welches ein starker, unsichtbarer, infraroter Laserstrahl in den Strahlengang eingekoppelt wird.

Sicherheitshinweis:

Der in diesem Experiment verwendete LASER besitzt die Laserschutzklasse 3B: Die zugängliche Laserstrahlung ist gefährlich für das Auge und für die Haut. Auch das Streulicht ist gefährlich.
Wenn der LASER eingeschaltet ist, müssen alle Personen im Raum geeigneten Laserschutzbrillen tragen!
Der direkte Blick in den Laser ist auch mit einer Laserschutzbrille strengstens untersagt!
Um den Laser sichtbar zu machen sind spezielle fluoreszierende Marker vorhanden.

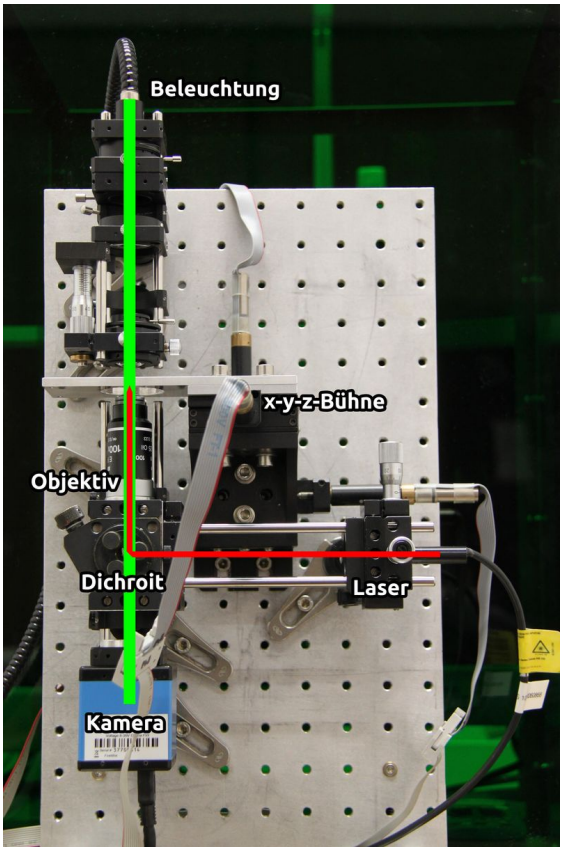

Abb. 3: Aubau des selbstgebauten Mikroskops auf dem optischen Tisch. Die Einkopplung des Lasers entfällt.

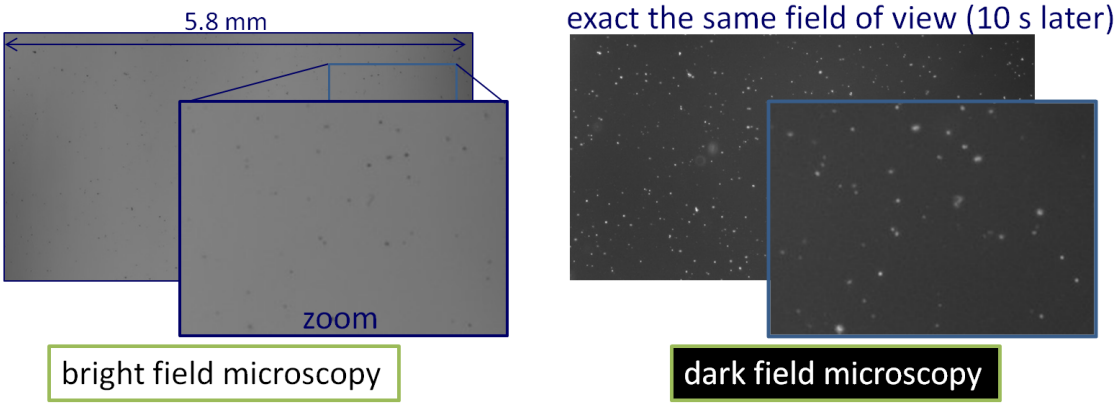

Abb. 4: Vergleich der Mikroskopbilder im Hellfeld (links) und Dunkelfeld (rechts). Es wurden 4 µm große Kügelchen mit einem 2-fach vergrößernden Objektiv beobachtet.

5. Durchführung der Experimente

5.1. Brown'sche Bewegung

Unter Anleitung werden Sie Proben mit kleinen Kügelchen präparieren. Sie werden eine Einführung in das verwendete Mikroskop und der Software zur Aufzeichnung von Bildsequenzen erhalten. Die Bildsequenzen werden von einem Matlab-Programm ausgewertet welches anschließend die Positionen $x(t_i), y(t_i)$ der Kügelchen in Pixel als Funktion der jeweiligen Bildnummer abspeichert. Daher müssen Sie vorweg mit einer Mikroskopskala die laterale Ausdehnung der Pixel beim gewählten Objektiv bestimmen, sowie die Framerate der Aufzeichnung notieren. Die abgespeicherten Trajektorien aus dem Matlab-Programm dienen dann als Ausgangspunkt zur statistischen Charakterisierung der Bewegung. Dazu werden das MSD(t) und an ausgewählten Zeitpunkten die $pdf(x;t)$ berechnet. Aus der Anpassung der MSD(t) Daten sollen der experimentelle Diffusionskoeffizient D_{exp} und die Driftgeschwindigkeit $\vec{v}_{\text{Drift}}$ der Kügelchen extrahiert werden. Durch gesonderte Betrachtung der x- bzw. y-Komponenten der Trajektorien ergeben sich die Komponenten der Driftgeschwindigkeit. Da die Diffusion isotrop ist, sollte D_{exp} für x und y Projektion der Trajektorien der gleiche sein. Ebenso sollen D_{exp} und $\vec{v}_{\text{Drift}}$ aus den $pdf(x,t_i)$ durch Anpassung an eine Gaußverteilung extrahiert werden. Deren einzige freien Parameter sind dabei der Schwerpunkt μ und die Varianz σ^2. Aus diesen können direkt die D_{exp} und $\vec{v}_{\text{Drift}}$ berechnet werden. Wenn dies für verschiedene Zeitpunkte t_i durchgeführt wird, erhalten Sie mehr Werte für D_{exp} und $\vec{v}_{\text{Drift}}$ und Sie bekommen so ein Gefühl für die Fehlergrenzen aus Ihren Daten.

Eine wichtige Eigenschaft der Brown'schen Molekularbewegung ist ihre Selbstähnlichkeit. Die Gaußkurven der $pdf(x,t_i)$ verbreitern sich mit wachsenden t_i. Wenn jedoch die Orte x mit der Zeit geeignet mit dem einzigen Parameter des Systems, dem Diffusionskoeffizienten D skaliert werden, so werden die pdf' zu einer Masterfunktion kollabieren:

$$\tilde{x} = x/\sqrt{2Dt_i} \tag{27}$$

$$\tilde{pdf}(\tilde{x};t_i) = \sqrt{2Dt_i}\, pdf(x/\sqrt{2Dt_i};t_i) \quad . \tag{28}$$

Da mit die Normierung der Wahrscheinlichkeitsdichte gewährleistet bleibt, muss eine Stauchung der pdf in x-Richtung mit einer Streckung in der Amplitude einher gehen.

5.1.1. Kamera kalibrieren

Zeichnen Sie zu Beginn ein Bild einer Mikrometerskala auf, damit Sie bei der abschließenden Auswertung die Pixelkoordinaten in µm umrechnen können.

5.1.2. Probenpräparation

Es stehen Lösungen mit Kügelchen verschiedener Größe zur Verfügung. Für die optimale Beobachtung und Auswertung der Kugelpositionen darf die Konzentration der Kugeln nicht zu hoch sein. Die Kügelchen sollten gut einzeln separierbar sein, dennoch sollte mindestens 50 im Blickfeld der Aufzeichnung sein um eine gute Statistik zu gewährleisten. Der Probenraum wird begrenzt von einem Objektträger und einem Deckgläsern, die mit Hilfe von doppelseitigem Klebeband auf einen Absctand von zirka 100 µm Abstand gehalten werden. Der Objektträger dient dabei als Träger. Durch das dünne Deckgläschen wird die Probe beobachtet. Mit Hilfe von Silikonfett wird das Austreten von Flüssigkeit verhindert.

5.2. Optische Pinzette

5.2.1. Kamera kalibrieren

Zeichnen Sie zu Beginn ein Bild einer Mikrometerskala auf, damit Sie bei der abschließenden Auswertung die Pixelkoordinaten in µm umrechnen können.

5.2.2. Leistung kalibrieren

1. Setzen Sie Laserschutzbrillen auf.
2. Platzieren Sie das Leistungsmessgerät im Strahlengang.
3. Nehmen Sie den Laser in Betrieb.
4. Mit Hilfe eines Matlab-Steuerung können Sie die relative Leistung des Lasers verändern.
5. Messen Sie die Leistung in W für verschiedene Regelamplituden in arb. Units.
6. Schalten Sie nach der Kalibrierung den Laser wieder aus.
7. Entfernen Sie das Leistungsmessgerät.

5.2.3. Bewegung in einem optischen Potential

Für die Handhabung der optischen Pinzette liegt eine ausführliche Anleitung am Arbeitsplatz.

1. Versiegeln Sie die Probe, sofern sich noch keine Luft zwischen den beiden Glasplatten befindet. Ist dies der Fall, präparieren Sie eine neue, vollständig versiegelte Probe.
2. Verwenden Sie das Ölimmersionsobjektiv mit 60-facher Vergrößerung. Vergessen Sie nicht, einen Tropfen Immersionsöl auf das Objektiv aufzubringen!
3. Beobachten Sie die Probe und fokussieren Sie auf den Boden der Probenkammer.
4. Nehmen Sie anschließend den Laser in Betrieb.
5. Fangen Sie eine freie Kugel mit der optischen Pinzette und positionieren Sie diese im Abstand von zirka 10 µm zum Boden.
6. Zeichnen Sie zirka eine Minute lang Bilder auf und benennen Sie den Datenordner aussagekräftig (Regelamplitude, Höhe über dem Boden). Führen Sie diese Messung für 10 verschiedene Laserleistungen durch. Beachten Sie, dass sich die Laserleistungen deutlich unterscheiden sollten. Die Kügelchen sollten sich aufgrund der thermischen Bewegung weiterhin in der Falle bewegen. Diese Art der Messung wird auch als stochastische Kalibrierung der Fallenstärke bekannt.
7. Entfernen Sie vorsichtig die Probe und danach das Objektiv und säubern Sie letzteres gründlich.

6. Ausarbeitung und Auswertung

Vorweg:
Wenn Sie Fragen haben, wenden Sie sich an uns, wir helfen gerne!

Ihre Ausarbeitung ist ein Praktikumsprotokoll mit eigenen experimentellen Daten und Auswertungen, kein Lehrbuch! Die Einleitung und die allgemeine Darstellung der Experimente soll sehr knapp -mit Ihren eigenen Wortengehalten sein. Vermeiden Sie Abschweifungen.

Bereits vor dem Beginn des experimentellen Teil des Versuches sollte bereits die Beantwortung (gerne auch Stichpunkte, Handskizzen, Bilder) der vorbereitenden Fragen abgeschlossen sein. Ebenso sollen die numerischen Simulationen bereits vorweg in die Ausarbeitung einfließen. Der Ergebnisteil wird nach der

Durchführung der Experimente und der Auswertung der Daten erstellt. Dieser sollte folgende Punkte enthalten:

- knappe Darstellung zur jeweiligen Umsetzung der Versuche, wie Bilder von Proben, des Aufbaus, eingestellte Parameter und so weiter
- bei der Brown'schen Bewegung im passiven und aktiven Fluid jeweils die MSD(t), ausgewählte $pdf(x, t_i)$ und die abgeleiteten Größen D_{exp} und v_{Drift}, führen Sie ebenfalls eine Fehlerbetrachtung durch. Diskutieren Sie die Unterschiede zwischen dem passiven und aktiven Fluid, hauptsächlich an den pdf'.
- die Ergebnisse zur Leistungskalibrierung des Lasers mit Einschätzung der Fehlerquellen
- die Bestimmung der Fallenstärke unter Verwendung der Methode der Kerndichteschätzer

Bitte zögern Sie nicht bei Verbesserungsvorschlägen zur Anleitung, einfach eine E-Mail an:
✉ thomas.john@physik.uni-saarland.de

7. Literaturverzeichnis

Literatur

[1] Jan K. G. Dhont. *An Introduction to Dynamics of Colloids*. Elsevier, 2003.

[2] Albert Einstein. Über die von der molekularkinetischen Theorie der Wärme geforderte Bewegung von in ruhenden Flüssigkeiten suspendierten Teilchen. *Annalen der Physik*, 322(8):549–560, 1905.

[3] E. M. Purcell. Life at low reynolds number. *American Journal of Physics*, 45:3–11, 1977.

Chapter 2

BROWNIAN MOTION OF NON-INTERACTING PARTICLES

2.1 Introduction

As discussed in the previous chapter, a colloidal particle exerts so-called Brownian motion due to thermal collisions with solvent molecules. This eratic motion can be described on the basis of Newton's equations of motion, where the interactions of the Brownian particle with the solvent molecules are taken into account by a rapidly fluctuating force. The statistics of Brownian motion can be studied in this way when reasonable approximations for the statistical properties of the fluctuating force can be made. We analyse in this chapter the translational Brownian motion of a single sphere, also in the presence of an externally imposed shear flow, and the translational and rotational motion of a long and thin rigid rod like particle.

A particular advantage of this approach is that it allows for a clear distinction of several time scales. As will turn out, the (angular) momentum coordinate of a Brownian particle relaxes to thermal equilibrium with the heat bath of solvent molecules within a time interval over which its position and orientation hardly change. This is a key feature of Brownian motion that offers the possibility to describe the statistics of displacements without involving the momentum coordinate. Especially for the treatment of interacting particles in later chapters this will turn out to be a very pleasant feature.

In the present chapter we are considering Brownian motion of non-interacting particles, that is, of Brownian particles which do not interact with other Brownian particles. This is the case for very dilute dispersions. Interactions of the Brownian particle with the solvent molecules must be fully accounted for, however, since these interactions drive the Brownian motion.

2.2 The Langevin Equation

Relaxation times for fluids are known experimentally to be of the order $10^{-14}s$. As will be established shortly, relevant time scales for Brownian particles are at least $10^{-9}s$. This separation in time scales is the consequence of the very large mass of the Brownian particle relative to that of a solvent molecule, and is essential for the validity of the Langevin description.

The interaction of the spherical Brownian particle with the solvent molecules is separated into two parts. First of all, there is a rapidly varying force $\mathbf{f}(t)$ with time t as the result of *random* collisions of solvent molecules with the Brownian particle. This force fluctuates on the forementioned solvent

time scale of $10^{-14}s$. Secondly, as the Brownian particle attains a velocity $\mathbf{v} = \mathbf{p}/M$ ($\mathbf{p}$ is the momentum coordinate of the Brownian particle and M its mass), there is a friction force due to *systematic* collisions with the solvent molecules. When the volume of the Brownian particle is much larger than that of the solvent molecules, this systematic force equals the hydrodynamic friction force of a macroscopically large sphere. For not too large velocities, that friction force is directly proportional to the velocity of the Brownian particle, and the proportionality constant γ is the friction constant: *friction force* $= -\gamma\,\mathbf{p}/M$. The friction coefficient of a macroscopically large sphere is shown in chapter 5 on hydrodynamics to be equal to,

$$\gamma = 6\pi\eta_0 a, \tag{2.1}$$

with η_0 the shear viscosity of the solvent and a the radius of the Brownian particle. The friction coefficient in eq.(2.1) is commonly referred to as Stokes's friction coefficient. Newton's equation of motion for a spherical Brownian particle is thus written as,

$$d\mathbf{p}/dt = -\gamma\,\mathbf{p}/M + \mathbf{f}(t). \tag{2.2}$$

The position coordinate $\mathbf{r}$ of the Brownian particle is, by definition, related to the momentum coordinate as,

$$d\mathbf{r}/dt = \mathbf{p}/M. \tag{2.3}$$

Since the systematic interaction with the solvent molecules is made explicit (the first term on the right-hand side of eq.(2.2)), the ensemble average of the fluctuating force $\mathbf{f}$ is equal to zero,

$$< \mathbf{f}(t) > = \mathbf{0}. \tag{2.4}$$

Due to the forementioned large separation in time scales, it is sufficient for the calculation of the thermal movement of the Brownian particle to use a delta correlated random force in time, that is,

$$< \mathbf{f}(t)\mathbf{f}(t') > = \mathbf{G}\,\delta(t-t'), \tag{2.5}$$

where δ is the delta distribution and $\mathbf{G}$ is a constant 3×3-dimensional matrix, which may be regarded as a measure for the strength of the fluctuating force, and is referred to as the *fluctuation strength*. Such a delta correlated random

force limits the description to a time resolution which is large with respect to the solvent time scale of $10^{-14}s$.

Equation (2.2) is Newton's equation of motion for a macroscopic particle with a fluctuating random force added to account for the thermal collisions of the solvent molecules with the Brownian particle. Such an equation is called a *Langevin equation*. It is a stochastic equation of motion in the sense that the momentum coordinate of the Brownian particle, as well as its position coordinate, are now stochastic variables. It makes no sense to ask for a deterministic solution of eqs.(2.2,3), since only ensemble averaged properties of the random force $\mathbf{f}$ are specified. The effort should be aimed at the calculation of the conditional probability density function for $\mathbf{p}$ and $\mathbf{r}$ at time t, given their initial values at time $t = 0$. Hereafter, "probability density function" is abbreviated as *pdf*. The solution of the Langevin equation is the specification of the pdf for the stochastic variable $(\mathbf{p}, \mathbf{r})$. Note that eq.(2.2) is mathematically meaningless as it stands without the specifications (2.4,5) of the statistical properties of the random force $\mathbf{f}$.

Integration of eq.(2.2) yields,

$$\mathbf{p}(t) = \mathbf{p}(0)\,\exp\{-\frac{\gamma}{M}t\} + \int_0^t dt'\,\mathbf{f}(t')\,\exp\{-\frac{\gamma}{M}(t-t')\}. \tag{2.6}$$

Now let τ be a time interval much larger than the solvent time scale of $10^{-14}s$. The random force evolves through many independent realizations during that time interval. On the other hand, let τ be so small that $\exp\{-\gamma t/M\}$ is almost constant over times of the order of τ, that is, we take $\tau \ll M/\gamma$. With this choice of τ, eq.(2.6) can be rewritten as,

$$\mathbf{p}(t) = \mathbf{p}(0)\,\exp\{-\frac{\gamma}{M}t\} + \sum_{j=0}^{N-1}\exp\{-\frac{\gamma}{M}(t-j\tau)\}\int_{j\tau}^{(j+1)\tau} dt'\,\mathbf{f}(t'), \tag{2.7}$$

where $N = t/\tau$. Since the random force evolves through many independent realizations during the time interval τ, each integral in eq.(2.7) is a Gaussian variable with a mean equal to zero. This is a consequence of the central limit theorem, as each integral may be regarded as a sum of many statistically equivalent and independent terms (the central limit theorem is formulated in (1.80) in the introductory chapter). Furthermore, since a sum of independent Gaussian variables is also a Gaussian variable, as shown in exercise 1.17 in chapter 1, it follows from the representation (2.7) that,

$$\mathbf{x_1} \equiv \mathbf{p}(t) - \mathbf{p}(0)\,\exp\{-\frac{\gamma}{M}t\},$$

is a Gaussian variable.

What about the position coordinate $\mathbf{r}$ of the Brownian particle? The above reasoning is easily extended to include the position coordinate. Using eq.(2.3), integration of eq.(2.6) yields (see exercise 2.1),

$$\begin{aligned} \mathbf{r}(t) &= \mathbf{r}(0) + \frac{\mathbf{p}(0)}{\gamma}\left[1-\exp\{-\frac{\gamma}{M}t\}\right] \\ &+ \frac{1}{\gamma}\int_0^t dt'\,\mathbf{f}(t')\left[1-\exp\{-\frac{\gamma}{M}(t-t')\}\right]. \end{aligned} \tag{2.8}$$

Following the same reasoning as before shows that,

$$\mathbf{x_2} \equiv \mathbf{r}(t) - \mathbf{r}(0) - \frac{\mathbf{p}(0)}{\gamma}\left[1-\exp\{-\frac{\gamma}{M}t\}\right],$$

is a Gaussian variable with a mean equal to zero.

Consider the stochastic variable $(\mathbf{p},\mathbf{r})$. Let us define the variable,

$$\begin{aligned} \mathbf{X} &\equiv (\mathbf{x_1},\mathbf{x_2}) \\ &= (\int_0^t dt'\,\mathbf{f}(t')\exp\{-\frac{\gamma}{M}(t-t')\} \\ &\quad ,\frac{1}{\gamma}\int_0^t dt'\,\mathbf{f}(t')\left[1-\exp\{-\frac{\gamma}{M}(t-t')\}\right]), \end{aligned} \tag{2.9}$$

where eqs.(2.6) and (2.8) are used in the second line. According to the above discussion, $\mathbf{X}$ is a Gaussian variable. For given initial values $\mathbf{p}(0)$ and $\mathbf{r}(0)$ of the momentum and position coordinates, the pdf of the variable $\mathbf{X}$ is clearly identical to the pdf of $(\mathbf{p},\mathbf{r})$. Hence, the pdf of $(\mathbf{p},\mathbf{r})$ is given by (for notation, see subsection 1.3.1 on conditional pdf's in the introductory chapter),

$$P(\mathbf{p},\mathbf{r},t \mid \mathbf{p}(0),\mathbf{r}(0),t=0) = \frac{1}{(2\pi)^{n/2}\sqrt{det\mathbf{D}}}\exp\{-\frac{1}{2}\mathbf{X}\cdot\mathbf{D^{-1}}\cdot\mathbf{X}\}, \tag{2.10}$$

with,

$$\mathbf{D} = <\mathbf{XX}> \equiv \begin{pmatrix} <\mathbf{x_1x_1}> & <\mathbf{x_1x_2}> \\ <\mathbf{x_2x_1}> & <\mathbf{x_2x_2}> \end{pmatrix}. \tag{2.11}$$

$det\mathbf{D}$ denotes the determinant of $\mathbf{D}$, and $n=6$ is the dimension of $\mathbf{X}$. Note that each of the matrices $<\mathbf{x_i x_j}>$, $i,j=1,2$, is 3×3-dimensional, so that $\mathbf{D}$ is 6×6-dimensional. Using eqs.(2.4,5), the ensemble averages $<\mathbf{x_i x_j}>$ are easily calculated,

$$<\mathbf{x_1x_1}> = \frac{M\mathbf{G}}{2\gamma}\left[1-\exp\{-\frac{2\gamma}{M}t\}\right], \tag{2.12}$$

$$<\mathbf{x_1x_2}> = <\mathbf{x_2x_1}> = \frac{M\mathbf{G}}{\gamma^2}\left[1-\exp\{-\frac{\gamma}{M}t\}\right]^2, \tag{2.13}$$

$$\begin{aligned} <\mathbf{x_2x_2}> &= \frac{M\mathbf{G}}{\gamma^3}(\frac{\gamma}{M}t - \frac{1}{2}\left[\exp\{-\frac{2\gamma}{M}t\}-1\right] \\ &\quad -2\left[1-\exp\{-\frac{\gamma}{M}t\}\right]). \end{aligned} \tag{2.14}$$

It is now possible to identify the matrix $\mathbf{G}$, using the equipartition theorem, which states that (see exercise 2.2),

$$\lim_{t\to\infty} <\mathbf{p}(t)\mathbf{p}(t)> = \hat{\mathbf{I}}\frac{M}{\beta}, \tag{2.15}$$

where $\beta = 1/k_BT$, with k_B Boltzmann's constant and T the temperature, and $\hat{\mathbf{I}}$ the unit matrix. The fluctuation strength now follows from the definition of the variable $\mathbf{x_1}$ (below eq.(2.7)) and the ensemble average (2.12). For times $t \gg M/\gamma$, eq.(2.12) reduces to,

$$<\mathbf{p}(t)\mathbf{p}(t)> = \mathbf{G}\frac{M}{2\gamma}. \tag{2.16}$$

Comparison with eq.(2.15) identifies the fluctuation strength,

$$\mathbf{G} = \hat{\mathbf{I}}\frac{2\gamma}{\beta}. \tag{2.17}$$

This relation is often referred to as a fluctuation dissipation theorem, because it connects the fluctuation strength with the friction coefficient, which determines the dissipation of kinetic energy into heat. With the identification of the fluctuation strength $\mathbf{G}$, the pdf of the Gaussian variable $(\mathbf{p},\mathbf{r})$ is completely specified.

2.3 Time Scales

In an experiment, the time scale is set by the time interval over which observables are averaged during a measurement. For example, taking photographs

of a Brownian particle is an experiment on a time scale which is set by the shutter time of the camera. Subsequent photographs reveal the motion of the Brownian particle averaged over a time interval equal to the shutter time. Any theory considering the motion of the Brownian particle obtained in such a way should of course be aimed at the calculation of observables, averaged over that time interval. A time scale is thus the minimum time resolution of an experiment or theory, and observables are averaged over the time interval that sets the time scale.

We have already introduced the solvent time scale in the previous section. The solvent time scale is of the order of the relaxation times for solvent coordinates, and is of the order $10^{-14}\ s$. The Langevin equation, together with the specifications (2.4,5) for the ensemble averages of the random force, is an equation that is valid on a time scale that is much larger than the solvent time scale. One might be tempted to set the random force $\mathbf{f}$ in the Langevin equation (2.2) equal to zero, since the average of $\mathbf{f}$ over a time interval equal to many times the solvent time scale is zero. However, the correlation function of $\mathbf{f}$ in eq.(2.5) is delta correlated, so that averages of products of the random force that appear on using the Langevin equation (2.2) cannot be set equal to zero. Thus, the random force on the right-hand side of eq.(2.2) must be retained. The coarsening in time is made explicit in the ensemble averages (2.4,5), while the original equations of motion (2.1,2) remain intact. The smallest time scale on which the specifications (2.4,5) for the averages of the random force make sense, is much larger than the solvent time scale. This time scale is usually referred to, for historical reasons, as the *Fokker-Planck time scale*, which we shall denote as τ_{FP}.

At the end of the previous section we have seen that the ensemble average $<\mathbf{p}(t)\mathbf{p}(t)>$ attains its equilibrium form for times $t \gg M/\gamma$. The momentum coordinate $\mathbf{p}$ thus relaxes on a time scale $\gg M/\gamma$. Consider now the full time dependence of $<\mathbf{p}(t)\mathbf{p}(t)>$. An explicit expression follows immediately from the definition of the variable $\mathbf{x_1}$ in the previous section (below eq.(2.7)) and the expression (2.12) for the average $<\mathbf{x_1}\mathbf{x_1}>$, together with the identification (2.17) of the fluctuation strength $\mathbf{G}$,

$$<\mathbf{p}(t)\mathbf{p}(t)>=\hat{\mathbf{I}}\frac{M}{\beta}\left[1-\exp\{-\frac{2\gamma}{M}t\}\right]+\mathbf{p}(0)\mathbf{p}(0)\exp\{-\frac{2\gamma}{M}t\}, \quad (2.18)$$

where, as before, $\hat{\mathbf{I}}$ is the unit matrix. For small times $\ll M/\gamma$ this becomes,

$$<\mathbf{p}(t)\mathbf{p}(t)>=\mathbf{p}(0)\mathbf{p}(0). \quad (2.19)$$

Hence, for these small times the Brownian particle did not yet change its velocity due to collisions with solvent molecules.

Let us now analyse the mean squared displacement as a function of time. The time dependent mean squared displacement follows immediately from the definition of the variable $\mathbf{x_2}$ in the previous section (just below eq.(2.8)) and the expression (2.14) for the average $<\mathbf{x_2}\mathbf{x_2}>$, together with the identification (2.17) of $\mathbf{G}$,

$$<(\mathbf{r}(t)-\mathbf{r}(0))(\mathbf{r}(t)-\mathbf{r}(0))>=\frac{\mathbf{p}(0)\mathbf{p}(0)}{\gamma^2}\left[\exp\{-\frac{\gamma}{M}t\}-1\right]^2 \quad (2.20)$$
$$+\hat{\mathbf{I}}\frac{2M}{\beta\gamma^2}\left(\frac{\gamma}{M}t-\frac{1}{2}\left[\exp\{-\frac{2\gamma}{M}t\}-1\right]-2\left[1-\exp\{-\frac{\gamma}{M}t\}\right]\right).$$

For times $t \gg M/\gamma$, this becomes,

$$<(\mathbf{r}(t)-\mathbf{r}(0))(\mathbf{r}(t)-\mathbf{r}(0))>=\hat{\mathbf{I}}\frac{2}{\beta\gamma}t. \quad (2.21)$$

The mean squared displacement thus varies linearly with time. This is quite different for ballistic motion, where the mean squared displacement would be proportional to t^2. The interpretation of this result is, that the Brownian particle suffered many random collisions with the solvent molecules, leading to many random changes of its velocity and thus reducing its displacement with time as compared to ballistic motion. Ballistic motion is observed for small times $t \ll M/\gamma$,

$$<(\mathbf{r}(t)-\mathbf{r}(0))(\mathbf{r}(t)-\mathbf{r}(0))>=\frac{\mathbf{p}(0)\mathbf{p}(0)}{M^2}t^2=\mathbf{v}(0)\mathbf{v}(0)\,t^2, \quad (2.22)$$

where $\mathbf{v}$ is the velocity of the Brownian particle. This equation is in accordance with eq.(2.19) : the velocity is not yet affected by collisions with solvent molecules for these small times, so that the displacement of the Brownian particle is simply linear with time.

For time scales $\gg M/\gamma$, the momentum coordinate is thus in equilibrium with the solvent, and the position coordinate changes, on average, proportional to $\sqrt{t}$. This time scale is usually referred to as the *Brownian, Diffusive*, or *Smoluchowski time scale*, which shall be denoted as τ_D. On that time scale a statistical description for the motion of the Brownian particle is feasible, without involving the momentum coordinate. We thus come to the following ordering of time scales,

$$10^{-14}s=\tau_{solvent}\ll\tau_{FP}\ll M/\gamma\ll\tau_D. \quad (2.23)$$

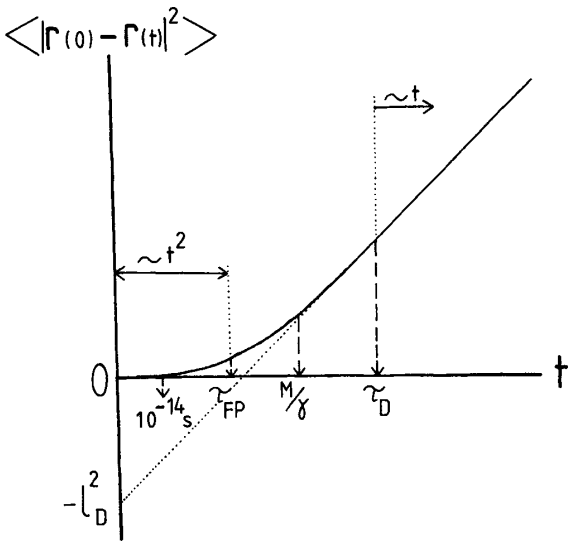

Figure 2.1:
The mean squared displacement $<|\ \mathbf{r}(t) - \mathbf{r}(0)\ |^2>$ *as a function of time.*

Using typical values for the mass and friction coefficient of a Brownian particle, one finds that $M/\gamma \approx 10^{-9} s$ (see exercise 2.3).

A statistical description on the solvent time scale involves the position and momentum coordinates of both the solvent molecules and the Brownian particles. On the Fokker-Planck time scale, the solvent coordinates are long relaxed to thermal equilibrium, and only the momentum and position coordinate of the Brownian particle need to be considered. Finally, on the Brownian or diffusive time scale, in addition, the momentum coordinate of the Brownian particles relaxed to equilibrium with the heat bath of solvent molecules, and a statistical description involving just the position coordinate of the Brownian particle is feasible.

A coarsening of the time scale implies a coarsening of the length scale. On the diffusive time scale the spatial resolution is not better than the distance over which the Brownian particle moves during a time interval equal to the diffusive time scale. The ensemble average of that distance, the *diffusive length scale* l_D, is easily obtained from eqs.(2.2,4). From these equations it

follows that,

$$< \mathbf{p}(t) > = \mathbf{p}(0)\ \exp\{-\frac{\gamma}{M}t\}, \tag{2.24}$$

so that,

$$l_D = \int_0^\infty dt\, \frac{|< \mathbf{p}(t) >|}{M} = |\ \mathbf{p}(0)\ |\ /\gamma. \tag{2.25}$$

A typical value for $|\ \mathbf{p}(0)\ |$ is obtained from the equipartition theorem,

$$|\ \mathbf{p}(0)\ | \approx \sqrt{<|\ \mathbf{p}\ |^2>} = \sqrt{3Mk_BT}. \tag{2.26}$$

The diffusive length scale is thus estimated as,

$$l_D \approx \sqrt{3Mk_BT}/\gamma = \sqrt{3Mk_BT}/6\pi\eta_0 a. \tag{2.27}$$

Typical values yield (see exercise 2.3),

$$\frac{l_D}{a} \approx 10^{-4} - 10^{-3}, \tag{2.28}$$

where a is the radius of the Brownian particle. The important conclusion is, that on the diffusive time scale the coarsening of the spatial resolution is only a tiny fraction of the size of the Brownian particle. *For the study of processes where a significant displacement of the Brownian particle is essential, a statistical description on the diffusive time scale is therefore sufficient.*

The results of the present section are summarized in fig.2.1, where the mean squared displacement is plotted as a function of time. For small times, that is, on the Fokker-Planck time scale, the mean squared displacement is proportional to t^2, eq.(2.22), whereas for large times, on the diffusive time scale, the mean squared displacement is linear in t, eq.(2.21). The linear curve in the diffusive regime intercepts the mean squared displacement axis for zero time at $-l_D^2$.

For non-interacting Brownian particles the diffusive time scale is the largest time scale of interest. As soon as interactions amongst Brownian particles come into play there are two further time scales. These two time scales are related to direct and hydrodynamic interactions between the Brownian particles and are referred to as the *interaction time scale* and the *hydrodynamic time scale*, respectively. These time scales are discussed in the chapters 4 and 5 on interacting particles and on hydrodynamics, respectively. The hydrodynamic time scale is of the same order as the diffusive time scale discussed here, while the interaction time scale can be much larger.

Before the pdf of the position coordinate is constructed (on the diffusive time scale) the method of solving the Langevin equation as discussed in section 2.2 is generalized in the following section.

2.4 Chandrasekhar's Theorem

Chandrasekhar's theorem is a generalization of the analysis of section 2.2 to arrive at the expression (2.10) for the pdf of $\mathbf{X}$. Instead of repeating the analysis of section 2.2 for each of the Langevin equations which are considered in the following sections, we discuss the general solution of these equations here once, and apply the resulting theorem to these special cases.

Let $\mathbf{X}$ be a m-dimensional stochastic variable, which obeys the following integrated Langevin equation,

$$\mathbf{X}(t) \;=\; \mathbf{\Phi}(t) + \int_0^t dt'\, \mathbf{\Psi}(t-t') \cdot \mathbf{F}(t'). \tag{2.29}$$

$\mathbf{\Phi}$ and the force $\mathbf{F}$ are both m-dimensional vectors and $\mathbf{\Psi}$ is a $m \times m$-dimensional matrix. Both $\mathbf{\Phi}$ and $\mathbf{\Psi}$ are deterministic and known functions of time. The stochastic force $\mathbf{F}$ is characterized by,

$$< \mathbf{F}(t) > = \; \mathbf{0}, \tag{2.30}$$

and,

$$< \mathbf{F}(t)\mathbf{F}(t') > = \; \mathbf{H}\,\delta(t-t'), \tag{2.31}$$

with $\mathbf{H}$ a constant $m \times m$-dimensional matrix. The conditional pdf of $\mathbf{X}$ at time t, given that its value is $\mathbf{\Phi}(t=0)$ at time $t=0$, is then given by,

$$\begin{aligned} P(\mathbf{X}, t \mid \mathbf{\Phi}(0), t=0) \;&=\; \frac{1}{(2\pi)^{m/2}\sqrt{det\mathbf{M}(t)}} \\ &\times \exp\left[-\frac{1}{2}(\mathbf{X}-\mathbf{\Phi}(t)) \cdot \mathbf{M}^{-1}(t) \cdot (\mathbf{X}-\mathbf{\Phi}(t))\right], \end{aligned} \tag{2.32}$$

where the $m \times m$-dimensional *covariance matrix* $\mathbf{M}(t)$ is defined as,

$$\mathbf{M}(t) \;\equiv\; \int_0^t dt'\, \mathbf{\Psi}(t') \cdot \mathbf{H} \cdot \mathbf{\Psi}^T(t'). \tag{2.33}$$

The dots here denote contraction of adjacent indices, that is, the ij^{th} element of $\mathbf{M}(t)$ is,

$$M_{ij}(t) \;=\; \sum_{p,q=1}^{m} \int_0^t dt'\, \Psi_{ip}(t')\, H_{pq}\, (\Psi^T)_{qj}(t'), \tag{2.34}$$

and the supersrcipt "T" stands for the "*transpose of* ". It is assumed here that the inverse of $\mathbf{M}(t)$ exists. This statement -Chandrasekhar's theorem- is established in precisely the same way as the expression (2.10) in section 2.2. According to eqs.(2.29) and (2.31), $\mathbf{X} - \mathbf{\Phi}(t)$ is a Gaussian variable for all times t (large enough, however, to ensure the validity of the delta correlation (2.31) of $\mathbf{F}$). The pdf for $\mathbf{X}$ can then be written down immediately, provided that the inverse of the matrix $\mathbf{M}(t)$ exists, since the pdf of $\mathbf{X} - \mathbf{\Phi}(t)$ is identical to that of $\mathbf{X}$.

For the case considered in section 2.1, we have, $\mathbf{X} = (\mathbf{x_1}, \mathbf{x_2})$, $\mathbf{F} = (\mathbf{f}, \mathbf{f})$, and both $\mathbf{\Phi}$ and $\mathbf{\Psi}$ follow immediately by comparison of the integrated Langevin equation (2.9) with eq.(2.29).

2.5 The pdf on the Diffusive Time Scale

The pdf of $\mathbf{r}$ on the diffusive time scale, where the momentum coordinate is in thermal equilibrium with the solvent, is obtained from Chandrasekhar's theorem and the integrated Langevin equation (2.8). Comparison of eq.(2.8) with eq.(2.29) and using eq.(2.17) for the fluctuation strength, yields, for times $t \gg M/\gamma$,

$$\begin{aligned} \mathbf{X} \;&\equiv\; \mathbf{r}, \\ \mathbf{\Phi} \;&\equiv\; \mathbf{r}(0) + \frac{\mathbf{p}(0)}{\gamma}, \\ \mathbf{F} \;&\equiv\; \mathbf{f}, \\ \mathbf{\Psi}(t) \;&\equiv\; \hat{\mathbf{I}}\frac{1}{\gamma}\left[1 - \exp\{-\frac{\gamma}{M}t\}\right], \\ \mathbf{H} \;&\equiv\; \hat{\mathbf{I}}\frac{2\gamma}{\beta}. \end{aligned} \tag{2.35}$$

The dimension m is 3 in this case. Note that the exponential time dependence of $\mathbf{\Psi}$ must be retained, even on the diffusive time scale, since in the integrated Langevin equation $\mathbf{\Psi}$ occurs as a function of $t - t'$, and t' ranges from 0 to t.

According to the above equalities and eq.(2.33), on the diffusive time scale, the matrix $\mathbf{M}(t)$ is given by,

$$\mathbf{M}(t) = \hat{\mathbf{1}} 2D_0 t, \tag{2.36}$$

where the *diffusion coefficient* D_0 is defined as,

$$D_0 = \frac{1}{\beta\gamma} = \frac{k_B T}{6\pi\eta_0 a}. \tag{2.37}$$

Such a relation between a diffusion coefficient and a friction coefficient is commonly referred to as an *Einstein* relation, and when an explicit expression for the friction coefficient is substituted it is referred as a *Stokes-Einstein* relation. Einstein and Stokes-Einstein relations apply also to rotational and translational diffusion of rigid rods, as will be seen in section 2.8. Chandrasekhar's theorem (2.32) thus yields,

$$P(\mathbf{r}, t \mid \mathbf{r}(0), t=0) = \frac{1}{(4\pi D_0 t)^{3/2}} \exp\left[-\frac{\mid \mathbf{r} - \mathbf{r}(0) - \frac{\mathbf{p}(0)}{\gamma} \mid^2}{4D_0 t}\right]. \tag{2.38}$$

In the previous section we have seen that on the diffusive time scale, the length scale is much larger than $\mid \mathbf{p}(0) \mid /\gamma$. The corresponding term in the exponential in the pdf of $\mathbf{r}$ is therefore meaningless, and should be omitted. For future reference we display here the more appropriate expression,

$$P(\mathbf{r}, t \mid \mathbf{r}(0), t=0)) = \frac{1}{(4\pi D_0 t)^{3/2}} \exp\left[-\frac{\mid \mathbf{r} - \mathbf{r}(0) \mid^2}{4D_0 t}\right]. \tag{2.39}$$

The physical meaning of the diffusion coefficient is that it sets the time required for significant displacements of the Brownian particle (see exercise 2.3).

2.6 The Langevin Equation on the Diffusive Time Scale

In arriving at the integrated Langevin equation (2.8) for the position coordinate $\mathbf{r}$ of the Brownian particle, we had to perform two integrations : a first integration of the equation of motion (2.2) for the momentum coordinate, and a second integration of the resulting integrated Langevin equation (2.6). The question is whether it is possible to coarsen the time scale right from

the beginning, on the level of the differential form of the Langevin equation. If possible, this would save the extra work involved in performing a second integration. For more complicated Langevin equations, like for rigid rod like Brownian particles (see the following sections), such a coarsening directly from the start saves a lot of work.

Since on the diffusive time scale the momentum coordinate is in thermal equilibrium with the solvent, one might guess that a coarsening at the level of the differential form of the Langevin equation (2.2) can be established simply by setting,

$$d\mathbf{p}/dt = 0, \tag{2.40}$$

that is, inertia of the Brownian particle is unimportant. It then follows that,

$$\mathbf{p}/M = \mathbf{f}(t)/\gamma, \tag{2.41}$$

so that a Langevin equation involving only the position coordinate is obtained from eq.(2.3),

$$d\mathbf{r}/dt = \mathbf{f}(t)/\gamma. \tag{2.42}$$

The corresponding integrated Langevin equation is thus simply,

$$\mathbf{r}(t) = \mathbf{r}(0) + \frac{1}{\gamma}\int_0^t dt' \mathbf{f}(t'). \tag{2.43}$$

Applying Chandrasekhar's theorem to this integrated Langevin equation immediately reproduces the pdf in eq.(2.39).

Equation (2.40) can be justified by simply rescaling the Langevin equation with respect to the coarsened time and length scales. The time scale we wish to work with here is the diffusive time scale $\tau_D \gg M/\gamma$, and the length scale is the diffusive length scale l_D as given in eq.(2.27). Defining the rescaled time and position,

$$t' = t/\tau_D\,, \tag{2.44}$$

$$\mathbf{r}' = \mathbf{r}/l_D\,, \tag{2.45}$$

the Langevin equations (2.2,3) are written as,

$$\frac{1}{\tau_D}\frac{M}{\gamma} d\mathbf{p}'/dt' = -\mathbf{p}' + \mathbf{f}', \tag{2.46}$$

$$d\mathbf{r}'/dt' = \frac{1}{M}\mathbf{p}', \tag{2.47}$$

where the rescaled momentum and stochastic force are defined as,

$$\mathbf{p}' = \frac{\tau_D}{l_D}\mathbf{p}, \tag{2.48}$$

$$\mathbf{f}' = \frac{M}{\gamma}\frac{\tau_D}{l_D}\mathbf{f}. \tag{2.49}$$

The primed variables are the variables in which we are interested when going to the coarsened description. The only thing we have done is to express time and position in new units, corresponding to the minimum resolution in the coarsened description. The factor that multiplies $d\mathbf{p}'/dt'$ in eq.(2.46) is very small, since $\tau_D \gg M/\gamma$. Therefore, the left hand-side of eq.(2.46) may be set equal to zero. This is the justification for eq.(2.40).

In the following sections, diffusion of spheres in shear flow and of rod like Brownian particles are considered. The corresponding Langevin equations are coarsened to diffusive time and length scales as described above, saving the considerable effort of solving the full Langevin equations.

2.7 Diffusion in Simple Shear Flow

Consider two flat plates with solvent contained in between. The plates are oppositely displaced, by means of external forces, with a constant speed (see fig.2.2). For not too large velocities of the plates, this induces a spatial linearly varying velocity of the solvent. For the coordinate system sketched in fig.2.2, the fluid flow velocity $\mathbf{u}_0$ is equal to,

$$\mathbf{u}_0(\mathbf{r}) = \boldsymbol{\Gamma}\cdot\mathbf{r}, \tag{2.50}$$

with,

$$\boldsymbol{\Gamma} = \dot{\gamma}\begin{pmatrix} 0 & 1 & 0 \\ 0 & 0 & 0 \\ 0 & 0 & 0 \end{pmatrix}, \tag{2.51}$$

where $\dot{\gamma}$ is called the *shear rate*, which is proportional to the velocity of the plates. The matrix $\boldsymbol{\Gamma}$ is the *velocity gradient matrix*. The fluid flow velocity as defined by eqs.(2.50,51) is called a *simple shear flow*.

Consider a Brownian particle immersed in a solvent which is in simple shear flow. The friction force is now not just equal to $-\gamma\mathbf{p}/M$. Instead of the absolute velocity of the Brownian particle, we have to use the velocity relative

Life at low Reynolds number

E. M. Purcell
Lyman Laboratory, Harvard University, Cambridge, Massachusetts 02138
(Received 12 June 1976)

Editor's note: This is a reprint (slightly edited) of a paper of the same title that appeared in the book *Physics and Our World: A Symposium in Honor of Victor F. Weisskopf*, published by the American Institute of Physics (1976). The personal tone of the original talk has been preserved in the paper, which was itself a slightly edited transcript of a tape. The figures reproduce transparencies used in the talk. The demonstration involved a tall rectangular transparent vessel of corn syrup, projected by an overhead projector turned on its side. Some essential hand waving could not be reproduced.

This is a talk that I would not, I'm afraid, have the nerve to give under any other circumstances. It's a story I've been saving up to tell Viki. Like so many of you here, I've enjoyed from time to time the wonderful experience of exploring with Viki some part of physics, or anything to which we can apply physics. We wander around strictly as amateurs equipped only with some elementary physics, and in the end, it turns out, we improve our understanding of the elementary physics even if we don't throw much light on the other subjects. Now this is that kind of a subject, but I have still another reason for wanting to, as it were, needle Viki with it, because I'm going to talk for a while about viscosity. Viscosity in a liquid will be the dominant theme here and you know Viki's program of explaining everything, including the heights of mountains, with the elementary constants. The viscosity of a liquid is a very tough nut to crack, as he well knows, because when the stuff is cooled by merely 40 degrees, its viscosity can change by a factor of a million. I was really amazed by fluid viscosity in the early days of NMR, when it turned out that glycerine was just what we needed to explore the behavior of spin relaxation. And yet if you were a little bug inside the glycerine, looking around, you wouldn't see much change in your surroundings as the glycerine cooled. Viki will say that he can at least predict the *logarithm* of the viscosity. And that, of course, is correct because the reason viscosity changes is that it's got one of these activation energy things and what he can predict is the order of magnitude of the exponent. But it's more mysterious than that, Viki, because if you look at the Chemical Rubber Handbook table you will find that there is almost no liquid with viscosity much lower than that of water. The viscosities have a big range *but they stop at the same place.* I don't understand that. That's what I'm leaving for him.[1]

Now, I'm going to talk about a world which, as physicists, we almost never think about. The physicist hears about viscosity in high school when he's repeating Millikan's oil drop experiment and he never hears about it again, at least not in what I teach. And Reynolds's number, of course, is something for the engineers. And the *low* Reynolds number regime most engineers aren't even interested in—except possibly chemical engineers, in connection with fluidized beds, a fascinating topic I heard about from a chemical engineering friend at MIT. But I want to take you into the world of very low Reynolds number—a world which is inhabited by the overwhelming majority of the organisms in this room. This world is quite different from the one that we have developed our intuitions in.

I might say what got me into this. To introduce something that will come later, I'm going to talk partly about how microorganisms swim. That will not, however, turn out to be the only important question about them. I got into this through the work of a former colleague of mine at Harvard, Howard Berg. Berg got his Ph.D. with Norman Ramsey, working on a hydrogen maser, and then he went back into biology which had been his early love, and into cellular physiology. He is now at the University of Colorado at Boulder, and has recently participated in what seems to me one of the most astonishing discoveries about the questions we're going to talk about. So it was partly Howard's work, tracking *E. coli* and finding out this strange thing about them, that got me thinking about this elementary physics stuff.

Well, here we go. In Fig. 1, you see an object which is moving through a fluid with velocity v. It has dimension a. In Stokes's law, the object is a sphere, but here it's anything; η and ρ are the viscosity and density of the fluid. The ratio of the inertial forces to the viscous forces, as Osborne Reynolds pointed out slightly less than a hundred years ago, is given by $av\rho/\eta$ or av/ν, where ν is called the *kinematic* viscosity. It's easier to remember its dimensions: for water, $\nu \approx 10^{-2}$ cm^2/sec. The ratio is called the Reynolds number and when that number is small the viscous forces dominate. Now there is an easy way, which I didn't realize at first, to see who should be interested in small Reynolds numbers. If you take the viscosity η and square it and divide by the density, you get a force (Fig. 2). No other dimensions come in at all. η^2/ρ is a force. For water, since $\eta \approx 10^{-2}$ and $\rho \approx 1$, $\eta^2/\rho \approx 10^{-4}$ dyn. That is a force that will tow *anything,* large or small, with a Reynolds number of order of magnitude 1. In other words, if you want to tow a submarine with Reynolds number 1 (or strictly speaking, $1/6\pi$ if it's a spherical submarine) tow it with 10^{-4} dyn. So it's clear in this case that you're interested in small Reynolds number if you're interested in *small forces* in an absolute sense. The only other people who are interested in low Reynolds number, although they usually don't have to invoke it, are the geophysicists. The Earth's mantle is supposed to have a viscosity of 10^{21} P. If you now work out η^2/ρ, the force is 10^{41} dyn. That is more than 10^9 times the gravitational force that half the Earth exerts on the other half! So the conclusion is, of course, that in the flow of the mantle of the Earth the Reynolds number is *very* small indeed.

Now consider things that move through a liquid (Fig. 3). The Reynolds number for a man swimming in water might be 10^4, if we put in reasonable dimensions. For a goldfish or a tiny guppy it might get down to 10^2. For the animals that we're going to be talking about, as we'll see in a moment, it's about 10^{-4} or 10^{-5}. For these animals inertia is totally irrelevant. *We* know that $F = ma$, but they could scarcely care less. I'll show you a picture of the real animals in a bit but we are going to be talking about objects which are the order of a micron in size (Fig. 4). That's a micron scale, not a suture, in the animal in Fig. 4. In water where the kinematic viscosity is 10^{-2} cm/sec these things move around with a typical speed of 30 μm/sec. If I have to push that animal to move it, and suddenly I stop pushing, how far will it coast before it slows down? The answer is, about 0.1 Å. And it takes it about 0.6 μsec to slow down. I think this makes it clear what low Reynolds number means. Inertia plays no role whatsoever. If you are at very low Reynolds number, what you are doing at the moment is entirely determined by the forces that are exerted on you *at that moment,* and by nothing in the past.[2]

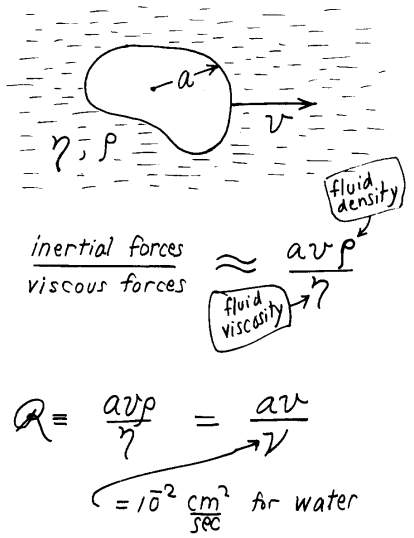

Figure 1.

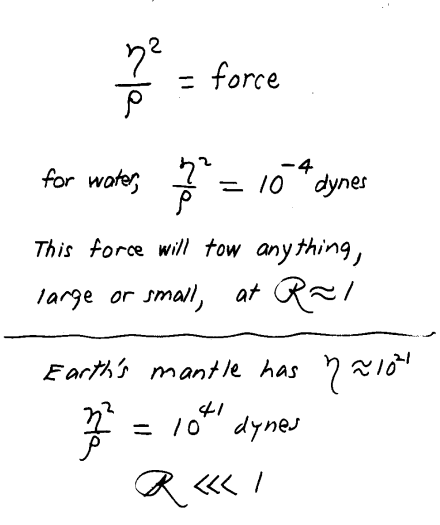

Figure 2.

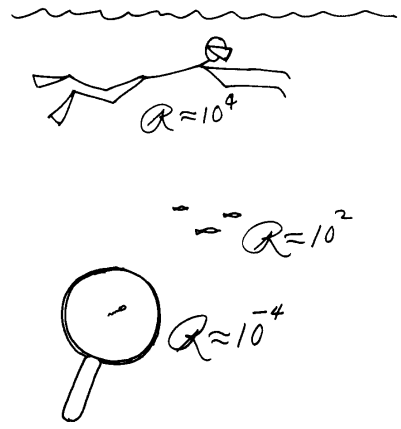

Figure 3.

It helps to imagine under what conditions a man would be swimming at, say, the same Reynolds number as his own sperm. Well, you put him in a swimming pool that is full of molasses, and then you forbid him to move any part of his body faster than 1 cm/min. Now imagine yourself in that condition: you're under the swimming pool in molasses, and now you can only move like the hands of a clock. If under those ground rules you are able to move a few meters in a couple of weeks, you may qualify as a low Reynolds number swimmer.

I want to talk about swimming at low Reynolds number in a very general way. What does it mean to swim? Well, it means simply that you are in some liquid and are allowed to deform your body in some manner. That's all you can do.

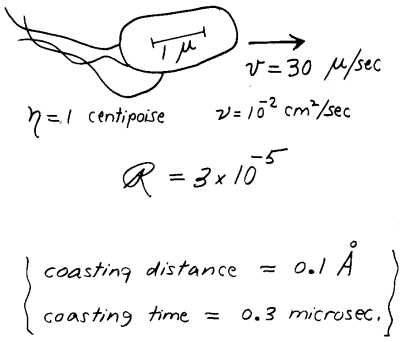

Figure 4.

This article is copyrighted as indicated in the article. Reuse of AAPT content is subject to the terms at: http://scitation.aip.org/termsconditions. Downloaded to IP: 134.96.37.149 On: Mon, 19 Oct 2015 06:24:12

Figure 5.

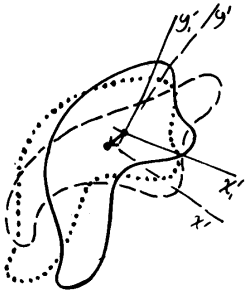

Move it around and move it back. Of course, you choose some kind of cyclic deformation because you want to keep swimming, and it doesn't do any good to use a motion that goes to zero asymptotically. You have to keep moving. So, in general, we are interested in cyclic deformations of a body on which there are no external torques or forces except those exerted by the surrounding fluid. In Fig. 5, there is an object which has a shape shown by the solid line; it changes its shape to the dashed contour and then it changes back. When it finally gets back to its original shape, the dotted contour, it has moved over and rotated a little. It has been swimming. When it executed the cycle, a displacement resulted. If it repeats the cycle, it will, of course, effect the same displacement, and in two dimensions we'd see it progressing around a circle. In three dimensions its most general trajectory is a helix consisting of little kinks, each of which is the result of one cycle of shape change.

There is a very funny thing about motion at low Reynolds number, which is the following. One special kind of swimming motion is what I call a reciprocal motion. That is to say, I change my body into a certain shape and then I go back to the original shape by going through the sequence in reverse. At low Reynolds number, everything reverses just fine. Time, in fact, makes no difference—only configuration. If I change quickly or slowly, the pattern of motion is exactly the same. If you take the Navier–Stokes equation and throw away the inertia terms, all you have left is $\nabla^2 v = p/\eta$, where p is the pressure (Fig. 6). So, if the animal tries to swim by a reciprocal motion, it *can't go anywhere.* Fast or slow, it exactly retraces its trajectory and it's back where it started. A good example of that is a scallop. You know, a scallop opens its shell slowly and closes its shell fast, squirting out water. The moral of this is that the scallop at low Reynolds number is no good. It can't swim because it only has one hinge, and if you have only one degree of freedom in configuration space, you are bound to make a reciprocal motion. There is nothing else you can do. The simplest animal that can swim that way is an animal with two hinges. I don't know whether one exists but Fig. 7 shows a hypothetical one. This animal is like a boat with a rudder at both front and back, and nothing else. This animal can swim. All it has to do is go through the sequence to configurations shown, returning to the original one at S_5. Its configuration space, of course, is two dimensional with coordinates θ_1, θ_2. The animal is going around a loop in that configuration space, and that enables it to swim. In fact, I worked this one out just for fun and you can prove from symmetry that it goes along the direction shown in the figure. As an exercise for the student, what is it that distinguishes that direction?

You can invent other animals that have no trouble swimming. We had better be able to invent them, since we know they exist. One you might think of first as a physicist, is a torus. I don't know whether there is a toroidal animal, but whatever other physiological problems it might face, it clearly could swim at low Reynolds number (Fig. 8). Another animal might consist of two cells which were stuck together and were able to roll on one another by having

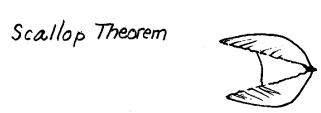

Figure 6.

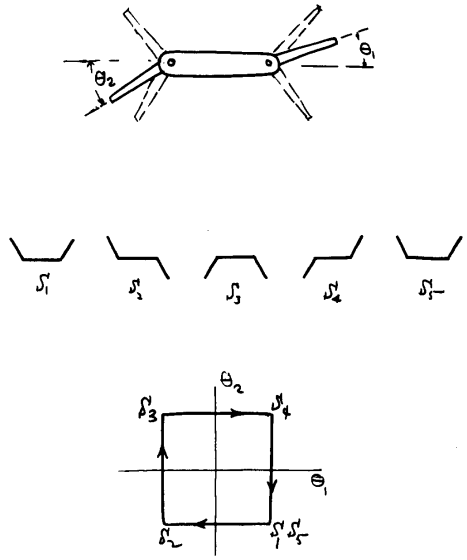

Figure 7.

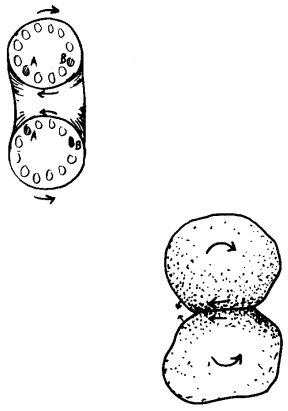

Figure 8.

some kind of attraction here while releasing there. That thing will "roll" along. I described it once as a combination caterpillar tractor and bicycle built for two, but that isn't the way it really works. In the animal kingdom, there are at least two other more common solutions to the problem of swimming at low Reynolds number (Fig. 9). One might be called the flexible oar. You see, you can't row a boat at low Reynolds number in molasses—if you are submerged—because the stiff oars are just reciprocating things. But if the oar is flexible, that's not true, because then the oar bends one way during the first half of the stroke and the other during the second half. That's sufficient to elude the theorem that got the scallop. Another method, and the one we'll mainly be talking about, is what I call a corkscrew. If you keep turning it, that, of course, is not a reciprocal change in configuration space and that will propel you. At this point, I wish I could persuade you that the direction in which this helical drive will move is *not* obvious. Put yourself back in that swimming pool under molasses and move around very, very slowly. Your intuitions about *pushing water backwards* are irrelevant. That's not what counts. Now, unfortunately, it turns out that the thing does move the way your naive, untutored, and actually incorrect argument would indicate, but that's just a pedagogical misfortune we are always running into.

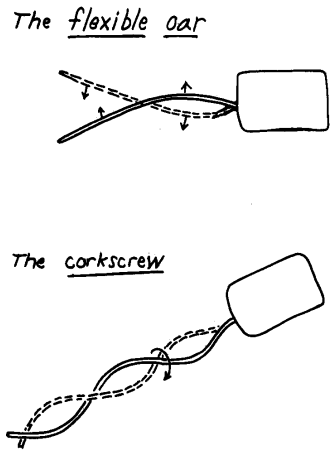

Figure 9.

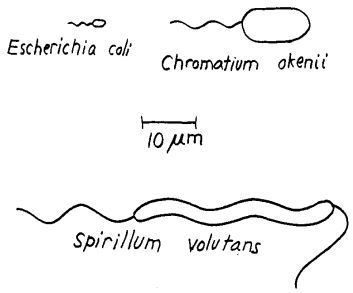

Figure 10.

Well, lets look at some real animals (Fig. 10). This figure I've taken from a paper of Howard Berg that he sent me. Here are three real swimmers. The one we're going to be talking about most is the famous animal, *Escherichia coli,* at A, which is a very tiny thing. Then there are two larger animals. I've copied down their Latin names and they may be old friends to some of you here. This thing (*S. volutans*) swims by waving its body as well as its tail and roughly speaking, a spiral wave runs down that tail. The bacterium *E. coli* on the left is about 2 μm long. The tail is the part that we are interested in. That's the flagellum. Some *E. coli* cells have them coming out the sides; and they may have several, but when they have several they tend to bundle together. Some cells are nonmotile and don't have flagella. They live perfectly well, so swimming is not an absolute necessity for this particular animal, but the one in the figure does swim. The flagellum is only about 130 Å in diameter. It is much thinner than the cilium which is another very important kind of propulsive machinery. There is a beautiful article on cilia in this month's *Scientific American.*[3] Cilia are about 2000 Å in diameter, with a rather elaborate apparatus inside. There's not room for such apparatus inside this flagellum.

For a long time there has been interest in how the flagellum works. Classic work in this field was done around 1951, as I'm sure some of you will remember, by Sir Geoffrey Taylor, the famous fluid dynamicist of Cambridge. One time I heard him give a fascinating lecture at the National Academy. Out of his pocket at the lecture he pulled his working model, a cylindrical body with a helical tail driven by a rubber-band motor inside the body. He had tested it in glycerine. In order to make the tail he hadn't just done the simple thing of having a turning corkscrew, because at that time nearly everyone had persuaded themselves that the tail doesn't rotate, it waves. Because, after all, to rotate you'd have to have a rotary joint back at the animal. So he had sheathed the turning helix with rubber tubing anchored to the body. The body had a keel. I remember Sir Geoffrey Taylor saying in his lecture that he was embarrassed that he hadn't put the keel on it first and he'd had to find out that

This article is copyrighted as indicated in the article. Reuse of AAPT content is subject to the terms at: http://scitation.aip.org/termsconditions. Downloaded to IP: 134.96.37.149 On: Mon, 19 Oct 2015 06:24:12

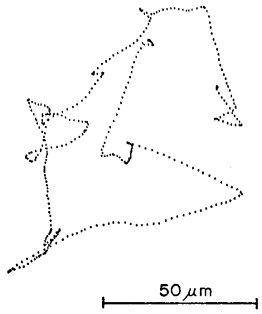

Figure 11.

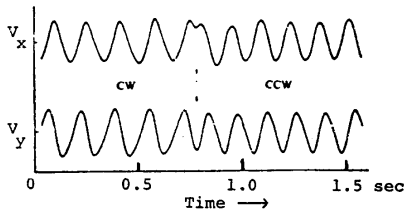

Figure 12.

ıe needed it. There has since been a vast literature on this ıubject, only a small part of which I'm familiar with. But ıt that time G. I. Taylor's paper in the *Proceedings of the Royal Society* could conclude with just three references: H. Lamb, *Hydrodynamics;* G. I. Taylor (his previous ɔaper); G. N. Watson, *Bessel Functions.* That is called ɡetting in on the ground floor.

To come now to modern times, I want to show a picture ɔf these animals swimming or tracking. This is the work of Howard Berg, and I'll first describe what he did. He started ɔuilding the apparatus when he was at Harvard. He was nterested in studying not the actual mechanics of swimming at all but a much more interesting question, namely, why these things swim and where they swim. In particular, ıe wanted to study chemotaxis in *E. coli*—seeing how they ɔehave in gradients of nutrients and things like that. So he ɔuilt a little machine which would track a single bacterium n *x, y, z* coordinates—just lock onto it optically and track t. He was able then to track one of these bacteria while it was behaving in its normal manner, possibly subject to the influence of gradients of one thing or another. A great advantage of working with a thing like *E. coli* is that there are so many mutant strains that have been well studied that you ɔan use different mutants for different things. The next picture (Fig. 11) is one of his tracks. It shows a projection ɔn a plane of the track of one bacterium. The little dots are about 0.1 sec apart so that it was actually running along one ɔf the legs for a second or two and the speed is typically 20–40 μm/sec. Notice that it swims for a while and then stops and goes off in some other direction. We'll see later what that might suggest. A year ago, Howard Berg went ɔut on a limb and wrote a paper in *Nature*[4] in which he argued that, on the basis of available evidence, *E. coli* must swim by *rotating* their flagella, not by waving them. Within the year a very elegant, crucial experiment by Silverman and Simon at UC–San Diego showed that this fact is the case.[5,6] Their experiment involved a mutant strain of *E. coli* bacteria which don't make flagella at all but only make something called the proximal hook to which the flagella would have been attached. They found that with antihook antibodies they could cause these things to glue together. And once in a while one of the bacteria would have its hook glued to the microscope slide, in which case the whole body rotated at constant angular velocity. And when two hooks glued together, the two bodies counter-rotated, as you would expect. It's a beautiful technique. Howard was ready with his tracker and the next picture[7] (Fig. 12) shows his tracker following the end of one of these tethered *E. coli* cells which is stuck to the microscope slide by antibody at the place where the flagellum should have been. Plotted here are the two velocity components V_x and V_y. The two velocity components are 90° out of phase. The point being tracked is going in a circle. In the middle of the figure, you see a 90° phase change in one component, a reversal of rotation. They can rotate hundreds of revolutions at constant speed and then turn around and rotate the other way. Evidently the animal actually has a rotary joint, and has a motor inside that's able to drive a flagellum in one direction or the other, a most remarkable piece of machinery.

I got interested in the way a rotating corkscrew can propel something. Let's consider propulsion in one direction only, parallel to the axis of the helix. The helix can translate and it can rotate; you can apply a force to it and a torque. It has a velocity v and an angular velocity Ω. And now remember, at low Reynolds number everything is linear. When everything is linear, you expect to see matrices come in. Force and torque must be related by matrices with constant coefficients, to linear and angular velocity. I call this little 2 × 2 matrix the propulsion matrix (Fig. 13). If I knew its elements *A, B, C, D,* I could then find out how good this rotating helix is for propelling anything.

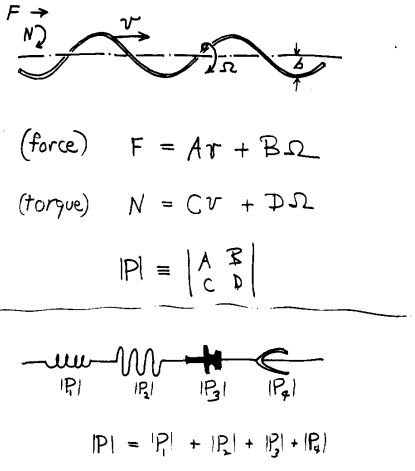

Figure 13.

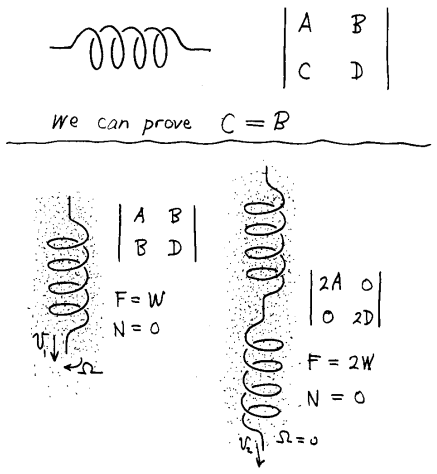

Figure 14.

Well, let's try to go on by making some assumptions. If two corkscrews or other devices on the same shaft are far enough from one another so that their velocity patterns don't interact, their propulsive matrices just add. If you allow me that assumption, then there is a very nice way, which I don't have time to explain, of proving that the propulsion matrix must be symmetrical (Fig. 14). So actually the motion is described by only three constants, not four, and they are very easily measured. All you have to do is make a model of this thing and drop in a fluid at you are interested in or not, because these constants are independent of that. And so I did that and that's my one demonstration. I thought this series of talks ought to have one experiment and there it is. We're looking through a tank not of glycerine but of corn syrup, which is cheaper, quite uniform, and has a viscosity of about 50 P or 5000 times the viscosity of water. The nice part of this is you can just lick the experimental material off your fingers.

Motion at low Reynolds number is very majestic, slow, and regular. You'll notice that the model is actually rotating but rather little. If that were a corkscrew moving through a cork of course, the pattern in projection wouldn't change. It's very very far from that, it's *slipping,* so that it sinks by several wavelengths while it's turning around once. If the matrix were diagonal, the thing would not rotate at all. So all you have to do is just see how much it turns as it sinks and you have got a handle on the off-diagonal element. A nice way to determine the other elements is to run two of these animals, one of which is a spiral and the other is two spirals, in series, of opposite handedness. The matrices add and with two spirals of opposite handedness, the propulsion matrix must be diagonal (Fig. 14). That's not going to rotate; it better not.

The propulsive efficiency is more or less proportional to the square of the off-diagonal element of the matrix. The off-diagonal element depnds on the difference between the drag on a wire moving perpendicular to its length and the drag on a wire moving parallel to its length (Fig. 15). These

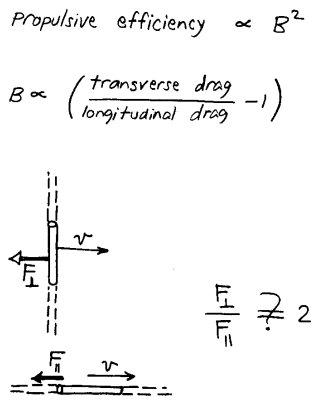

Figure 15.

are supposed to differ in a certain limit by a factor of 2. But for the models I've tested that factor is more like 1.5. Since it's that factor minus 1 that counts, that's very bad for efficiency. We thought that if you want something to rotate more while sinking, it would be better not to use a round wire. Something like a slinky ought to be better. I made one and measured its off diagonal elements. Surprise, surprise, it was no better at all! I don't really understand that, because the fluid mechanics of these two situations is not at all simple. In each case there is a logarithmic divergence that you have to worry about, and the two are somewhat different in character. So that theoretical ratio of two I referred to is probably not even right.

When you put all this in and calculate the efficiency, you find that it's really rather low even when the various parameters of the model are optimized. For a sphere which is driven by one of these helical propellers (Fig. 16), I will

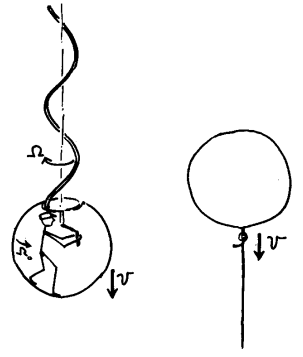

Figure 16.

This article is copyrighted as indicated in the article. Reuse of AAPT content is subject to the terms at: http://scitation.aip.org/termsconditions. Downloaded to IP: 134.96.37.149 On: Mon, 19 Oct 2015 06:24:12

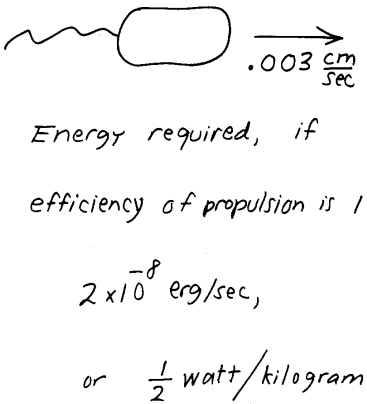

Figure 17.

define the efficiency as the ratio of the work that I would have to do just to pull that thing along to what the man inside it turning the crank has to do. And that turns out to be about 1%. I worried about that result for a while and tried to get Howard interested in it. He didn't pay much attention to it, and he shouldn't have, because it turns out that efficiency is really not the primary problem of the animal's motion. We'll see that when we look at the energy requirement. How much power does it take to run one of these things with a 1% efficient propulsion system, at this speed in these conditions? We can work it out very easily. Going 30 μm/sec, at 1% efficiency will cost us about 2×10^{-8} ergs/sec at the motor. On a per weight basis, that's a 0.5 W/kg, which is really not very much. Just moving things around in our transportation system, we use energy at 30 or 40 times that rate. This bug runs 24 h a day and only uses 0.5 W/kg. That's a small fraction of its metabolism and its energy budget. Unlike us, they do not squander their energy budget just moving themselves around. So they don't care whether they have a 1% efficient flagellum or a 2% efficient flagellum. It doesn't really make that much difference. They're driving a Datsun in Saudi Arabia.

So the interesting question is not how they swim. Turn anything—if it isn't perfectly symmetrical, you'll swim. If the efficiency is only 1%, who cares. A better way to say it is that the bug can collect, by diffusion through the surrounding medium, enough energetic molecules to keep moving when the concentration of those molecules is 10^{-9} M. I've now introduced the word diffusion. Diffusion is important because of another very peculiar feature of the world at low Reynolds number, and that is, stirring isn't any good. The bug's problem is not its energy supply; its problem is its environment. At low Reynolds number you can't shake off your environment. If you move, you take it along; it only gradually falls behind. We can use elementary physics to look at this in a very simple way. The time for transporting anything a distance l by stirring, is about l divided by the stirring speed v. Whereas, for transport by diffusion, it's l^2 divided by D, the diffusion constant. The ratio of those two times is a measure of the effectiveness of stirring versus that of diffusion for any given distance and diffusion constant. I'm sure this ratio has someone's name but I don't know the literature and I don't know whose number that's called. Call it S for *stirring number*.[8] It's just lv/D. You'll notice by the way that the Reynolds number was lv/ν. ν is the kinematic viscosity in cm^2/sec, and D is the diffusion constant in cm^2/sec, for whatever it is that we are interested in following—let us say a nutrient molecule in water. Now, in water the diffusion constant is pretty much the same for every reasonably sized molecule, something like 10^{-5} cm^2/sec. In the size domain that we're interested in, of micron distances, we find that the stirring number S is 10^{-2}, for the velocities that we are talking about (Fig. 18). In other words, this bug can't do anything by stirring its local surroundings. It might as well wait for things to diffuse, either in or out. The transport of wastes away from the animal and food to the animal is entirely controlled locally by diffusion. You can thrash around a lot, but the fellow who just sits there quietly waiting for stuff to diffuse will collect just as much.

At one time I thought that the reason the thing swims is that if it swims it can get more stuff, because the medium is full of molecules the bug would like to have. All my instincts as a physicist say you should move if you want to scoop that stuff up. You can easily solve the problem of diffusion in the velocity field represented by the Stokes flow around a sphere—for instance, by a relaxation method. I did so and found out how fast the cell would have to go to increase its food supply. The food supply if it just sits there is $4\pi aND$ molecules/sec, where a is the cell's radius (Fig. 19) and N is the concentration of nutrient molecules. To increase its food supply by 10% it would have to move at a speed of 700 μm/sec, which is 20 times as fast as it can swim. The increased intake varies like the square root of the bug's velocity so the swimming does no good at all in that respect. But what it can do is find places where the food is better or more abundant. That is, it does not move like a cow

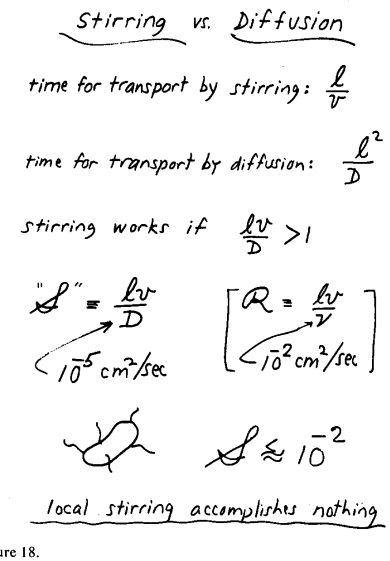

Figure 18.

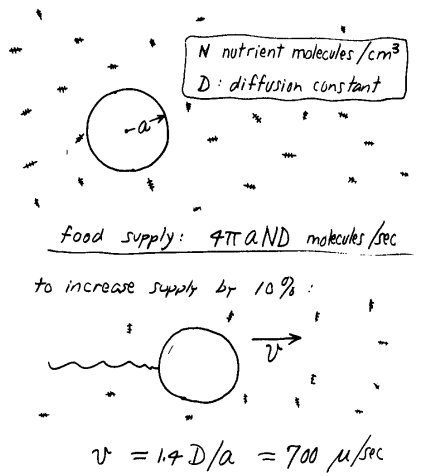

Figure 19.

that is grazing a pasture—it moves to find *greener pastures*. And how far does it have to move? Well, it has to move far enough to outrun diffusion. We said before that stirring wouldn't do any good locally, compared to diffusion. But suppose it wants to run over there to see whether there is more over there. Then it must outrun diffusion, and how do you do that? Well, you go that magic distance, D/v. So the rule is then, to outswim diffusion you have to go a distance which is equal to or greater than this number we had in our S constant. For typical D and v, you have to go about 30 μm and that's just about what the swimming bacteria were doing. If you don't swim that far, you haven't gone anywhere, because it's only on that scale that you could find a

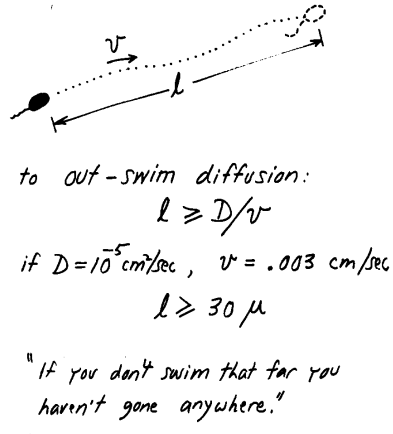

Figure 20.

difference in your environment with respect to molecules of diffusion constant D (Fig. 20).

Let's go back and look at one of those sections from Berg's track (Fig. 11). You'll see that there are some little trips, but otherwise you might ask why did it go clear over here and stop. Why did it go back? Well, my suggestion is, and I'd like to put this forward very tentatively, that the reason it does is because it's trying to outrun diffusion. Otherwise, it might as well sit still, as indeed do the mutants who don't have flagella. Now there is still another thing that I put forward with even more hesitation because I haven't tried this out on Howard yet. When he did his chemotaxis experiments, he found a very interesting behavior. If these things are put in a medium where there is a gradient of something that they like, they gradually work their way upstream. But if you look at how they do it and ask what rules they are using, what the algorithm is to use the current language, for finding your way upstream, it turns out that it's very simple. The algorithm is: if things are getting better, don't stop so soon. If, in other words, you plot, as Berg has done in some of his papers, the distribution of path lengths between runs and the little stops that he calls "twiddles," the distribution of path lengths if they are going *up* the gradient gets longer. That's a very simple rule for working your way to where things are better. If they're going down the gradient, though, they don't get shorter. And that seems a little puzzling. Why, if things are getting worse, don't they change sooner? My suggestion is that there is no point in stopping sooner. There is a sort of bedrock length which outruns diffusion and is useful for sampling the medium. Shorter paths would be a ridiculous way to sample. It may be something like that, but as I say, I don't know. The residue of education that I got from this is partly this stuff about simple fluid mechanics, partly the realization that the mechanism of propulsion is really not very important except, of course, for the physiology of that very myserious motor, which physicists aren't competent even to conjecture about.

I come back for a moment to Osborne Reynolds. That was a very great man. He was a professor of engineering, actually. He was the one who not only invented Reynolds number, but he was also the one who showed what turbulence amounts to and that there is instability in flow, and all that. He is also the one who solved the problem of how you lubricate a bearing, which is a very subtle problem that I recommend to anyone who hasn't looked into it. But I discovered just recently in reading in his collected works that toward the end of his life, in 1903, he published a very long paper on the details of the *submechanical universe*, and he had a complete theory which involved small particles of diameter 10^{-18} cm. It gets very nutty from there on. It's a mechanical model, the particles interact with one another and fill all space. But I thought that, incongruous as it may have seemed to put this kind of stuff in between our studies of the submechanical universe today, I believe that Osborne Reynolds would not have found that incongruous, and I'm quite positive that Viki doesn't.

[1](1976 footnote) As no one will be surprised to hear, Professor Weisskopf has recently shown me how this can be explained. I hope he will communicate it to AJP readers.

[2](1976 footnote) In that world, Aristotle's mechanics is *correct!* See A. Franklin, Am. J. Phys. **44**, 527–528 (1976).

This article is copyrighted as indicated in the article. Reuse of AAPT content is subject to the terms at: http://scitation.aip.org/termsconditions. Downloaded to IP: 134.96.37.149 On: Mon, 19 Oct 2015 06:24:12

[3]P. Satir, Sci. Am. **231,** 45 (October 1974).
[4]H. C. Berg and R. A. Anderson, Nature **245,** 380 (1973).
[5]M. Silverman and M. Simon, Nature **249,** 73 (1974).
[6]S. H. Larson, R. W. Reader, E. N. Kort, W-W. Tso, and J. Adler, Nature **249,** 74 (1974).
[7]H. C. Berg, Nature **249,** 77 (1974).
[8]I've recently discovered that its official name is the *Sherwood number*, so *S* is appropriate, after all! There is a list of all the dimensionless ratios that have acquired names—an astonishingly long list—in the *McGraw-Hill Encyclopedia of Science and Technology* (1971).

BIBLIOGRAPHY OF RECENT REVIEW ARTICLES

H. C. Berg, Nature **254,** 389 (1975).
H. C. Berg, Ann. Rev. Biophys. Biolog. **4,** 119 (1975).
J. Adler, Ann. Rev. Biochem. **44,** 341 (1975).
H. C. Berg, Sci. Am. **233,** 36 (August 1975).

TEACHING

So how do you go about teaching them something new? By mixing what they know with what they don't know. Then, when they see vaguely in their fog something they recognize, they think, "Ah, I know that." And then it's just one more step to, "Ah, I know the whole thing." And their mind thrusts forward into the unknown and they begin to recognize what they didn't know before and they increase their powers of understanding.

—Picasso, in *Life with Picasso* by Francoise Gilot and Carlton Lake (Nelson, London, 1965), p. 66.

Statistics of Colloidal Suspensions Stirred by Microswimmers

Levke Ortlieb,[1] Salima Rafaï,[2] Philippe Peyla,[2] Christian Wagner,[1] and Thomas John[1,*]

[1] *Universität des Saarlandes, Postfach 151150, D-66041 Saarbrücken, Germany*
[2] *LIPhy, CNRS et University J. Fourier, Grenoble France*

(Dated: November 6, 2018)

We present a statistical analysis of experimental trajectories of micron sized colloids in a dilute suspension of the green algae *Chlamydomonas reinhardtii*. The probability density function of displacements covers seven orders of magnitude and can be described by a convolution of two Gaussian distributions. The central peak results from classical thermal Brownian motion and the non-Gaussian long time tail is caused by single microswimmers. Still, we find that the mean squared displacements of tracer positions is linear over the complete measurement time interval. Experiments are performed for various tracer diameters, swimmer concentrations and mean swimmer velocities. This allows a rigorous comparison with existing theoretical models. We can exclude a description based on an effective temperature and other mean field approaches that describe the irregular motion as a sum of the fluctuating far field of many microswimmers. Our data are in many respects best described by the microscopic model by Thiffeault, PRE **92** 023023(2015).

Microscopic unicellular algae are abundant in the earth's oceans, rivers and lakes. They are crucial for the ecosystem since they have an estimated contribution of 50% to the world's oxygen production [1, 2]. In addition, it is suspected that they play an important role in stirring the top level of the oceans [3–6]. This so called biogenetic mixing is important for the availability of nutrients for many organisms. In the presence of active microswimmers, a passive fluid is stirred and shows an *active* spatio-temporal random fluid motion. These fluctuations at the scale of microorganisms can be characterized by tracking suspended tracer particles such as microspheres [7]. They undergo both Brownian thermal motion and follow the active random fluid motion generated by swimmers. Seminal work with this technique was presented by Wu and Libchaber in 2000 [8] with a study on concentrated *E. coli* bacteria suspensions. They report a non-Brownian, superdiffusive behavior of the mean squared displacement $MSD(t)$ for short time intervals, but the tracers were much bigger compared to the bacteria. In 2009, Leptos et al. [9] presented experimental data on diffusing microspheres in a dilute suspensions of the swimming algae *Chlamydomonas reinhardtii* (CR). In this case, the tracers were of comparable size to the microswimmers. CR are so called puller swimmers and have become a standard for this type of microswimmers in many laboratory experiments [10]. Leptos et al. observed a linear $MSD(t)$ of the tracer positions with a *diffusive scaling*, that could be rescaled by their standard deviation and remain self-similar, although PDFs were non-Gaussian. One class of models that could show such behavior are continuous time random walks (CTRW)[11]. Some theoretical predictions suggest that the scaling of the distribution function is transient and disappears for longer time measurements [12]. These experiments were followed by several further experiments on biological microswimmers [13], artificial swimmers [14, 15] and several theoretical models were presented [11, 12, 16–20]. We followed the experimental concept of Leptos et al. [9] up to a point where statistical significance allowed us to exclude several theoretical and phenomenological explanations and descriptions. Furthermore, we can conclusively answer a key question: Until which time scales can the enhanced diffusivity be described by the short time interactions between single swimmers and tracers? Therefore, we will analyze (a) the mean squared displacement MSD of trajectories of tracer particles with various diameters and for two different swimmer velocities (b) the non-Gaussian shape of the probability density function $pdf(x;t)$ at a fixed time difference and (c) the temporal propagation of the *pdf* and its kurtosis in order to quantify for the non-Gaussianity and the break down of *diffusive scaling* as proposed in Ref. [12].

Experiments were performed with an Eclipse TE-2000-S Nikon microscope with a 4× objective (NA = 0.2) and a Flea3 FL3-U3-88S2C-CMOS-camera recording at 60 Hz with a resolution of 2048 px × 1080 px. This relatively small magnification results in a very large field of view (1.56 mm×0.82 mm) and depth of field (more than 50 µm) so we can follow the 2D projection of the 3D motion of hundreds of tracers in focus for several minutes which is favorable for good statistics compared to a more precise determination of the position with a higher magnification [21]. The suspensions were observed in microscopy chambers (ibidi®, µ-Slide VI 0.4) with a thickness of 400 µm in the direction of gravity and a lateral extension of 3.8 mm × 17 mm. The middle of the chamber was in focus to exclude boundary effects. The specific swimmer number density was determined immediately before performing an experiment by counting the swimmers in self made chambers of 60 µm height. At our low number densities, miscounts due to overlapping could be excluded but due to sample inhomogeneities and local density variations, the maximal error in swimmer number densities has to be estimated to be up to 25%. The observation was in done in dark field. A red light source

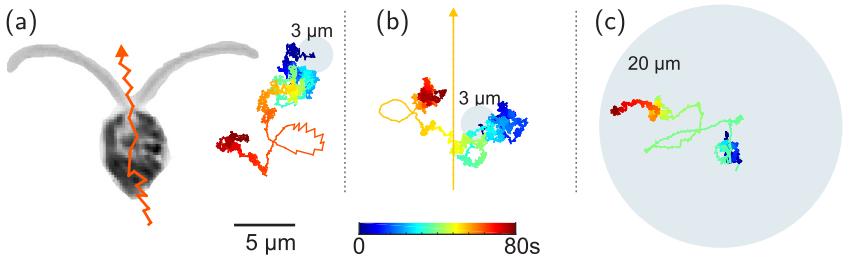

Figure 1. A picture of a microswimmer in (a) and tracer trajectories taken over Δt = 80 s. Colors refer to time and the sketched microspheres and the swimmer are to scale. (a) Trajectories of microswimmer and the microsphere at the moment of short range interaction (around $t \approx 70$ s). At this time interval the irregular Brownian motion of the tracer is superimposed by a loop.(b) Simulated trajectory of a Brownian microsphere with a similar loop at $t \approx 60$ s due to a passing spherical squirmer [12] with a velocity of $U = 35$ µm/s moving along the direction of the arrow. (c) Trace of a much bigger sphere interacting at $t \approx 40$ s. In this case the Brownian motion is less pronounced but the size of the loop is comparable to (a) and (b).

($\lambda > 600$ nm) was used for illumination at low intensities because the strain of CR (WT.T222-mt+ and SAG 11-32c-mt) are phototactic for shorter wave lengths. We took special care to obtain almost identical body diameters of the CR of approximately 10 µm by appropriate breeding. All cells were in the same stage of their life cycle. The algae are grown in TAP-medium at a temperature $T = (296 \pm 1)$ K and the viscosity of the suspending medium is $\eta = (0.95 \pm 0.1)$ mPas [22]. The mean swimming speeds of the strain WT.T222 mt+ and SAG 11-32c-mt- was $U = (35 \pm 10)$ µm/s and (70 ± 20) µm/s respectively. The latter has a faster flagella beat and is referred to as "fast swimmer" in the following. We use mono-disperse ($\sigma < 5\%$) uncoated polystyrene microspheres with diameters d between 1 µm and 20 µm as tracers (Fluka/Sigma Aldrich). They have a density of 1.05 g/cm^3 and for experiments with beads larger than 3 µm a density matching with a suitable mixture of water and same amount of heavy water (D_2O) was necessary to avoid sedimentation. In these experiments, the algae were grown in TAP medium, and heavy water was added shortly before the experiment. The swimming speed of the algae in the solution with D_2O did not change compared to the standard solution within an hour, but the algae did not survive for more than a few hours. The slight viscosity increase due to the heavy water $\eta_{D_2O+H_2O}/\eta_{H_2O} > 1$ is taken into account as correction for the effective diffusion coefficient for direct comparison with experiments in the standard solution. The diffusion coefficient for Brownian motion is given by the Stokes-Einstein relation $D_0 = k_B T/(6\pi\eta R)$ with tracer radius R and temperature T. To extract the trajectories from image sequences we use a MATLAB® based software developed in our group [21, 23]. The sup-pixel resolution of 0.1 µm of tracer positions is achieved by intensity weighted centroid determination.

Figure 1 shows trajectories of two tracer particles of different sizes at the moment in time when a swimmer passes close by. Thermal noise results in a typical Brownian motion and the according random displacements are proportional to the size of the particle. During the short time interval when the swimmer is close to the tracer, the latter performs a large, looped motion Fig. 1(a). According to Ref. [12, 24], those loops are the major contribution for the observed enhanced diffusivity. Note that with our setup we were not able to observe that a tracer was carried by a swimmer over long distances as described in Ref. [13] since we cannot resolve tracers too close to the swimmer. The duration of the interaction of a tracer with a swimmer is only parts of a second and small compared to the full trajectory. This is visualized in Fig. 1(b) showing a simulation of a tracer trajectory with a passing swimmer modeled as a squirmer. A squirmer is a model of an active moving sphere in Stokes flow. The so called squirmer parameter β defines if the flow field is comparable to a a pusher or puller [25]. We reproduced the simulations described in Ref. [12] and added Brownian noise. In contrast to Brownian motion, the size of the loops due to passing swimmers is independent of the size of the tracer, see Fig. 1(c).

Figure 2(a) shows the $MSDs$ in the $x-y$ plane. They were extracted by taking the time average for each trajectory followed by an ensemble average (see [21, 26]). In this way a significant improved statistics can be achieved. We find a perfect linear dependency $MSD \propto t$ over almost three orders of magnitude for all particle diameters, swimmer number densities and swimmer velocities. Only at short time intervals $t < 0.1$ s, the MSD deviates slightly from the linear slope due to uncorrelated position detection noise [26, 27]. Due to this linearity, an effec-

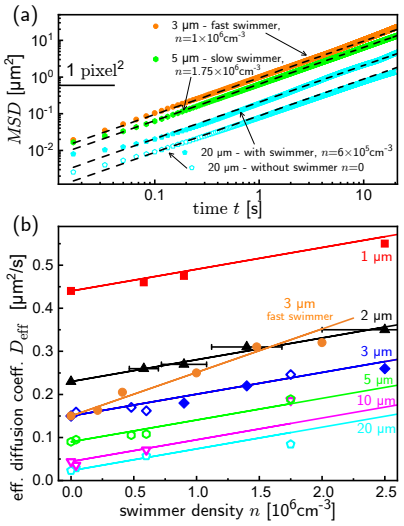

Figure 2. (a) Mean squared displacements MSD for various tracers diameter in suspensions of slow, fast and without swimmers (b) Effective diffusion coefficients vs. the swimmer number density n for various tracer diameters d for slow swimmers and one example for fast swimmers. For particles with a diameter $d \geq 3\,\mu$m D_2O was added to the TAP solution to prevent sedimentation (open symbols). Lines correspond to predictions by Eq. (1). Error bars in swimmer densities are only shown for the 2 µm tracers.

tive diffusion coefficient can be defined as the slope (the offset in double logarithmic axes) $MSD(t) = 2d\,D_{\rm eff}\,t$, in the case of $d = 2$ spatial dimensions. The fitted effective diffusion coefficients $D_{\rm eff}$ a function of the measured swimmer number density n are shown in Fig. 2(b). Lines represent the diffusion coefficients as predicted for a squirmer model in Ref. [12] (Eq. (27)):

$$D_{\rm eff} = D_0 + \left(0.266 + \frac{3}{4}\pi\beta\right) U n \ell^4 \qquad (1)$$

U is the mean swimmer velocity , $\ell = 6\,\mu$m the radius of the squirmer and $\beta = 0.6$ the fitted squirmer parameter. A positive $\beta > 0$ refers to a puller swimmer. In our experiments, the Einstein-Stokes diffusion coefficients D_0 without swimmers agree with the measured value in the range of few percent. The good quantitative agreement of measured and predicted $D_{\rm eff}(n)$ from Eq. (1) confirms that the increment of the diffusion coefficient $D_{\rm eff} - D_0$ is independent from the tracer size. In any case, all lines from the strain with the same mean velocity U have the same slope. For the fast strain with a double mean

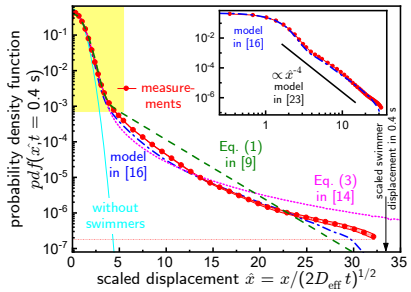

Figure 3. Experimental $pdf(\hat{x}, t = 0.4\,\mathrm{s})$ (–●–) at a number density of $n = 1.5 \times 10^6\,\mathrm{cm}^{-3}$ for a particle diamater of $d = 3\,\mu$m. The red shadowed regions indicated the 95% bootstrap confidence interval [32]. Several theoretical models are shown: (- - -) a superposition of Gaussian and Exponential from Ref. [9], (···) CTRW-model and (-·-) the microscopic model by Thiffeault [12], see text for parameters. The measured pdf for a pure Brownian motion is shown as (—). The yellow area indicates the data range presented in [9]. The inset shows the same data on double logarithmic axes to confirm the prediction $pdf \propto \hat{x}^{-4}$ by Ref. [24]. The black arrow indicates the scaled maximum distance of the microswimmer within 0.4s.

swimming speed, the slope is also doubled, according to Eq.(1). Therefore, we can exclude characterizations where $D_{\rm eff}$ is associated with an effective temperature like $k_{\rm B}T_{\rm eff} = 6\pi\eta R D_{\rm eff}(n)$ [8, 28–31]. An effective temperature definition also requires a Maxwell-Boltzmann distribution, however, we observed a non-Gaussian probability density function pdf for the displacements.

The probability density function $pdf(x;t)$ of tracer displacements contains more informations than the MSD, the second moment $MSD(t) = \int x^2 pdf(x;t)\mathrm{d}x$ of the distribution. Figure 3 shows an exemplary pdf from an experimental data set of length 300 s with approximately 5×10^4 (partially fragmented) trajectories with all together 3×10^7 data points. A local adaptive kernel density estimator is used to estimate the empirical pdf [33]. Only the right part of the pdf is shown because it is symmetric. The spatial dimension is nondimensionalized $\hat{x} = x/(2D_{\rm eff}t)^{1/2}$ according to the *diffusive scaling* as in Ref. [9]. At this low number density of $n = 1.5 \times 10^6\,\mathrm{cm}^{-3}$ the mean inter-swimmer distance is 90 µm and we can exclude any collective motion. The presented data set covers more than six orders of magnitude which strongly extends the data range presented in [9] (cp. the yellow area in Fig. 3). This allows us to compare our data with predictions from various models, in particular with respect to the non-Gaussian tails on a logarithmic axis. The central part of the pdf is always a Gaussian, caused only by the thermal motion of the tracers. The inset in

Fig. 3 shows that the $pdf \propto \hat{x}^{-4}$ has a power law tail as predicted by Pushkin and Yeomans in Ref. [24, Eq.(12)] for dipolar swimmers such as CR in 3D. This behavior is also predicted by the microscopic model by Thiffeault [12]. Leptos et al. in [9] fit their data with a superposition of a Gaussian and an Exponential, i.e. a parabola and a straight line in a semi logarithmic plot [34]. Fig. 3 shows that this does not describe the non-Gaussianity of the pdf well. Eckhard et al. [11] suggested a description in terms of a continuous time random walk (CTRW). One remarkable feature of a CTRW is that it is possible to construct random paths with a linear MSD in time but with a non-Gaussian pdf. The CTRW presented in Ref. [11] predicts a self similarity of the pdf by proper scaling of space and time. Such a self similarity was already observed by Leptos et al. and referred to as *diffusive scaling* comparable to pure Brownian motion in Ref. [9]. If we fit the relevant equation (3) in Ref. [11] to our $\log(pdf)$ to minimize relative differences [35]. The predicted pdf deviates slightly from our experimental data, in particular at the far end of the tails. The reason is that the swimmers move a maximum distance of approximately 15 µm in the considered time interval of 0.4 s. This gives an estimate of the maximum tracer displacement caused by passing of a single swimmer. The empirical pdf decreases quicker when approaching this length scale $U \times t$ than predicted. However, although the experimental statistics can be adjusted with a MSD and pdf from a CTRW. However, simulated random walks of a CTRW model have never loops as observed in the swimmer experiment, see Fig. 1.

At longer time intervals, several swimmer-tracer interactions result in larger, statistically independent displacements. According to the central limit theorem the sum of many displacements yields a Gaussian pdf. The convolution of two Gaussian pdfs, one from thermal and one from swimmer contributions, is still a Gaussian. This means that for long times the enhanced diffusing coefficient $D_{\rm eff}$ should persists. The collapse of the *diffusive scaling* at $t \gtrapprox 2$ s is shown in Fig. 4. For longer intervals t_i the pdf evolves towards a Gaussian with a larger diffusion coefficient compared to Brownian motion. By way of contrast, the CTRW approach includes an intrinsic self-similarity for all times.

We compare our data with the microscopic model by Thiffeault [12] which models the swimmers as squirmers with a fixed speed U, a radius ℓ and the squirmer parameter β. The first two parameters were chosen by fitting Eq.(1) to our experimental data. The calculated pdf is in very good accordance with our measurements (Fig. 3). The model contains an intrinsic maximal length scale $U \times t$. However, for displacements close to this length scale the experimental probability decays slightly slower than predicted. A possible explanation could be the broad speed distribution of the swimmers. Events with larger displacements could be caused by swimmers moving faster than the mean swimming speed U.

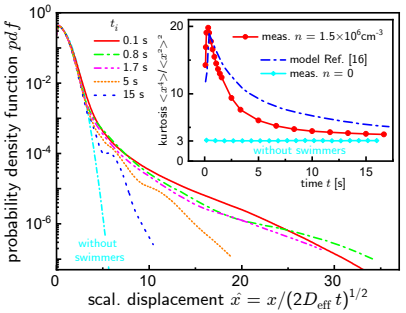

Figure 4. Experimental pdf at $n = 1.5 \times 10^6\,\mathrm{cm}^{-3}$ for various time intervals t_i to visualize the breakdown of the *diffusive scaling*. The pdf becomes a Gaussian for $t_i > 2$ s as predicted in [12]. The inset shows the kurtosis as measure to quantify the non Gaussian tails.

In accordance with our measurements (Fig. 4), the model by Thiffeault predicts the breakdown of the diffusive scaling, i.e. a transition from a non-Gaussian to a Gaussian pdf for longer times. Therefore, the pdfs cannot be scaled to collapse. However, the MSD is still linear throughout our measurements (cp. chapter VI in [12]). A good measure to quantify the deviation from a Gaussian pdf is the kurtosis κ, the fourth standardized moment, shown in the inset of Fig. 4. Both experimental kurtosis and the kurtosis calculated from the model by Thiffeault agree reasonably well. The kurtosis is very sensitive to the long tails of the distribution and again the broad swimmer speed distribution might explain the remaining discrepancy. The peak in the kurtosis at 0.2 s indicates the interaction time of a tracer with a passing swimmer. As expected, experiments without swimmers have a time independent $\kappa = 3$. The heuristic approach in [9] as sum of Gaussian and Exponential is time invariant and predicts a fixed $\kappa = 3.55$ for $f = 0.04$. The pdf of a CTRW decays as a power law [36] with exponent lower than four so the kurtosis does not exist.

In conclusion, we have shown that the enhanced diffusion of tracer particles in an environment of microswimmers is governed by rare events of single swimmers passing close by, leading to a tracer displacement in the form of loops. The spatial pdf covers seven orders of magnitude which allows us to compare our data to several theoretical models. We find that the microscopic model by Thiffeault [12] describes our data best. For intermediate times, the diffusive behavior can be scaled to a master curve but the scaling breaks down for longer times.

We gratefully acknowledge C. Ruloff, A. Morozov, and S. Zammert for stimulating discussions.

* thomas.john@physik.uni-saarland.de

[1] Christopher B. Field, Michael J. Behrenfeld, James T. Randerson, and Paul Falkowski, "Primary production of the biosphere: integrating terrestrial and oceanic components," Science **281**, 237–240 (1998).

[2] Jeffrey S Guasto, Roberto Rusconi, and Roman Stocker, "Fluid mechanics of planktonic microorganisms," Annual Review of Fluid Mechanics **44**, 373–400 (2012).

[3] Monica M. Wilhelmus and John O. Dabiri, "Observations of large-scale fluid transport by laser-guided plankton aggregationsa)," Physics of Fluids **26**, 101302 (2014).

[4] Eric Kunze, John F. Dower, Ian Beveridge, Richard Dewey, and Kevin P. Bartlett, "Observations of biologically generated turbulence in a coastal inlet," Science **313**, 1768–1770 (2006).

[5] André W. Visser, "Biomixing of the oceans?" Science **316**, 838–839 (2007).

[6] A. M. Leshansky and L. M. Pismen, "Do small swimmers mix the ocean?" Physical Review E **82**, 025301 (2010).

[7] E. M. Furst, *Microrheology* (Oxford University Press, 2017).

[8] Xiao-Lun Wu and Albert Libchaber, "Particle diffusion in a quasi-two-dimensional bacterial bath," Physical Review Letters **84**, 3017 (2000).

[9] Kyriacos C Leptos, Jeffrey S Guasto, Jerry P Gollub, Adriana I Pesci, and Raymond E Goldstein, "Dynamics of enhanced tracer diffusion in suspensions of swimming eukaryotic microorganisms," Physical Review Letters **103**, 198103 (2009).

[10] E. H. Harris, D. B. Stern, and G. B. Witman, eds., *The Chlamydomonas Sourcebook* (Academic Press, 2009).

[11] Bruno Eckhardt and Stefan Zammert, "Non-normal tracer diffusion from stirring by swimming microorganisms," The European Physical Journal E **35**, 1–2 (2012).

[12] Jean-Luc Thiffeault, "Distribution of particle displacements due to swimming microorganisms," Physical Review E **92**, 023023 (2015).

[13] Raphaël Jeanneret, Dmitri O. Pushkin, Vasily Kantsler, and Marco Polin, "Entrainment dominates the interaction of microalgae with micron-sized objects," Nature Communications **7**, 12518 (2016).

[14] Aidan Brown and Wilson Poon, "Ionic effects in self-propelled pt-coated janus swimmers," Soft Matter **10**, 4016–4027 (2014).

[15] Sébastien Michelin and Eric Lauga, "Geometric tuning of self-propulsion for Janus catalytic particles," Scientific Reports **7**, 42264 (2017).

[16] Zhi Lin, Jean-Luc Thiffeault, and Stephen Childress, "Stirring by squirmers," Journal of Fluid Mechanics **669**, 167–177 (2011).

[17] Alexander Morozov and Davide Marenduzzo, "Enhanced diffusion of tracer particles in dilute bacterial suspensions," Soft Matter **10**, 2748 (2014).

[18] Eric W. Burkholder and John F. Brady, "Tracer diffusion in active suspensions," Physical Review E **95**, 052605 (2017).

[19] Vittoria Sposini, Aleksei V. Chechkin, Flavio Seno, Gianni Pagnini, and Ralf Metzler, "Random diffusivity from stochastic equations: Comparison of two models for Brownian yet non-Gaussian diffusion," New Journal of Physics **20**, 043044 (2018).

[20] Blaise Delmotte, Eric E Keaveny, Eric Climent, and Franck Plouraboué, "Simulations of Brownian tracer transport in squirmer suspensions," IMA Journal of Applied Mathematics **83**, 680 (2018).

[21] Christian L. Vestergaard, "Optimizing experimental parameters for tracking of diffusing particles," Phys. Rev. E **94**, 022401 (2016).

[22] Elizabeth H Harris, *The Chlamydomonas sourcebook: introduction to Chlamydomonas and its laboratory use*, Vol. 1 (Academic Press, 2009).

[23] Brendan P. Marsh, Nagaraju Chada, Raghavendar Reddy Sanganna Gari, Krishna P. Sigdel, and Gavin M. King, "The Hessian Blob Algorithm: Precise Particle Detection in Atomic Force Microscopy Imagery," Scientific Reports **8**, 978 (2018).

[24] Dmitri O. Pushkin and Julia M. Yeomans, "Fluid mixing by curved trajectories of microswimmers," Physical review letters **111**, 188101 (2013).

[25] M. J. Lighthill, "On the squirming motion of nearly spherical deformable bodies through liquids at very small Reynolds numbers," Communications on Pure and Applied Mathematics **5**, 109–118 (1952).

[26] Xavier Michalet, "Mean square displacement analysis of single-particle trajectories with localization error: Brownian motion in an isotropic medium," Phys. Rev. E **82**, 041914 (2010).

[27] Thierry Savin and Patrick S Doyle, "Static and dynamic errors in particle tracking microrheology," Biophysical journal **88**, 623–638 (2005).

[28] Jérémie Palacci, Cécile Cottin-Bizonne, Christophe Ybert, and Lydéric Bocquet, "Sedimentation and Effective Temperature of Active Colloidal Suspensions," Physical Review Letters **105** (2010), 10.1103/PhysRevLett.105.088304.

[29] Davide Loi, Stefano Mossa, and Leticia F. Cugliandolo, "Effective temperature of active matter," Phys. Rev. E **77**, 051111 (2008).

[30] M. C. Marchetti, J. F. Joanny, S. Ramaswamy, T. B. Liverpool, J. Prost, Madan Rao, and R. Aditi Simha, "Hydrodynamics of soft active matter," Reviews of Modern Physics **85**, 1143–1189 (2013).

[31] Alison E. Patteson, Arvind Gopinath, Prashant K. Purohit, and Paulo E. Arratia, "Particle diffusion in active fluids is non-monotonic in size," Soft Matter **12**, 2365–2372 (2016).

[32] David W. Scott, *Multivariate density estimation: theory, practice, and visualization* (John Wiley & Sons, 2015).

[33] Hideaki Shimazaki and Shigeru Shinomoto, "Kernel bandwidth optimization in spike rate estimation," Journal of Computational Neuroscience **29**, 171–182 (2010).

[34] Note that the superposition of two independent random processes, e.g. thermal noise and random swimmer induced displacements, results in a convolution of the corresponding *pdf*s. The assumption of a superposition is only a functional approximation without an underlying model. Our fit parameters for Equation (1) in Ref. [9] are $f = 0.024$; $A_g = 0.65\,\mu\mathrm{m\,s}^{-1/2}$ and $A_e = 1.82\,\mu\mathrm{m\,s}^{-1/2}$.

[35] Different from stated in [11], two parameters are required, the α and the fractional D in units of $\mu\mathrm{m}^{2\alpha}\mathrm{s}^{-\alpha}$. The time can not be scaled out as claimed. We obtain the parameters $\alpha = 0.975$ and $D = 0.22\,\mu\mathrm{m}^{2\alpha}\mathrm{s}^{-\alpha}$.

[36] Bartłomiej Dybiec and Ewa Gudowska-Nowak, "Subordinated diffusion and continuous time random walk asymptotics," Chaos: An Interdisciplinary Journal of Nonlinear Science **20**, 043129 (2010).